ANALOGIES BETWEEN EM AND ACOUSTIC WAVES*

By

H. S. Hayre and G. Vroulis

TR-68-19

Department of Electrical Engineering
Wave Propagation Laboratories

UNIVERSITY OF HOUSTON
Cullen College of Engineering
3801 Cullen Boulevard
Houston, Texas 77004

November, 1968

*This work is sponsored by NASA Manned Spacecraft Center, Houston, Texas, under Contract NAS 9-7828.

Introduction

The purpose of this report is to summarize the results of a considerable amount of work in the field of acoustic simulation of radar return so that the reader may be readily confident about the validity of this inexpensive laboratory tool.

Acoustic simulation readily permits experimental verification of scatter theories which would otherwise be costly and time consuming.

Wave Equations

Electromagnetic	Acoustic
$\nabla \times E = -\mu \frac{\partial H}{\partial t}$	$\nabla P = -\rho_l \frac{\partial u}{\partial t}$
$\nabla \times H = \epsilon \frac{\partial E}{\partial t}$	$\nabla \cdot u = -K_l \frac{\partial P}{\partial t}$

for plane sinusoidal waves in the x-direction:

$\frac{dEy}{dx} = -i\omega\mu Hz$	$\frac{dP}{dx} = -i\omega\rho_l un$
$\frac{dHz}{dx} = -i\omega\epsilon Ey$	$\frac{du_x}{dx} = -i\omega K_l P$

taking the divergence of (1) and the substitution of (2)

$\nabla^2 E = \mu\epsilon \frac{\partial^2 E}{\partial t^2}$	$\nabla^2 P = \rho_l K_l \frac{\partial^2 P}{\partial t^2}$
$\nabla^2 H = \mu\epsilon \frac{\partial^2 H}{\partial t^2}$	$\nabla^2 u = \rho_l K_l \frac{\partial^2 u}{\partial t^2}$

where

E = electric field vector	P = pressure field scalar
H = magnetic field vector	u = particle velocity vector
ϵ = dielectric constant	ρ_l = density of the medium
μ = permeability	K_l = compressibility of medium

Simulation of electromagnetic waves using acoustic waves is always feasible when their respective boundary conditions are nearly the same.

BOUNDARY CONDITIONS

Electromagnetic

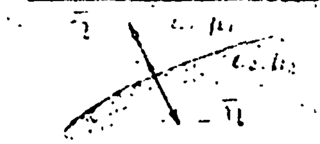

Most General Form

$\bar{n} \times (\bar{E}_1 - \bar{E}_2) = Q$ (1)

$\bar{n} \times (\bar{H}_1 - \bar{H}_2) = J_s$ (2)

When:

M_1/M_2 = Dielectric/Dielectric	$Q = 0$ $J_s = 0$
M_1/M_2 = Dielectric/Perf. Cond. $\sigma = \infty$ $\bar{E}_2 = \bar{H}_2 = 0$	$Q \neq 0$ $J_s = 0$
M_1/M_2 = Dielectric/Imp. Cond. σ = finite	$Q \neq 0$ $J_2 = 0$
M_1/M_2 = Perfect Conductor/Imp. Cond. $\bar{E}_1 = \bar{H}_2 = 0$	$Q \neq 0$ $J_s \neq 0$

Acoustic

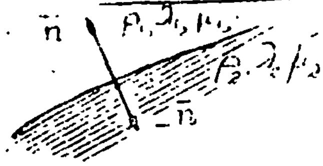

Most General Form

$P_1 = P_2$ (1)

$\bar{n} . (\bar{U}_1 - \bar{U}_2) = 0$ (2)

When:

M_1/M_2 = Liquid/Liquid	$P_1 = P_2$ $\bar{n} . (\bar{U}_1 - \bar{U}_2) = 0$
M_1/M_2 = Liquid/Solid Rigid	$P_1 = P_2 = 0$ $\bar{n} . (\bar{U}_1 - \bar{U}_2) = 0$
M_1/M_2 = Liquid/Semielastic Solid	$P_1 = P_2 = 0$ $U_{total} = U_t = 2U_{incident}$
M_1/M_2 = Solid/Elastic Rigid Solid	$P_1 = P_2 = 0$ $\bar{n} . (\bar{U}_1 - \bar{U}_2) = 0$

Conductors

Perfect Conductor:	$\sigma \to \infty$
Imperfect Conductor:	σ = finite
Insulator:	$\sigma = 0$

Solid Surfaces

Rigid Surface:	$\mu \Rightarrow \infty$
Elastic Surface:	μ = finite
Liquid Surface:	$\mu = 0$

For the EM and, Acoustic field $\bar{n}$ is a unit vector normal to the surface. The equations state that the tangential components of $\bar{E}$ and $\bar{H}$ are continuous across the boundary as are the pressure P and the normal component of the particle velcoity $\bar{\ }$.

Boundary conditions at a perfect conductor require the tangential electric field to be zero and the tangential magnetic field to be two times the incident field. On the other hand at a perfectly elastic wall (pressure release surface) the dynamic pressure is zero and the normal component of the total particle velocity is twice the normal component of the incident particle velocity. In each of these situations there is no wave propagation beyond the interface.

When a plane electromagnetic wave is normally incident on a perfectly conducting plane surface, the field components are both parallel to the surface and the electric field component can be made equivalent to either the pressure of the particle velocity in the acoustic wave using a perfectly elastic boundary in the first case and a perfectly rigid boundary in the second.

SCATTERING FROM A CYLINDER

Electromagnetic	Acoustic
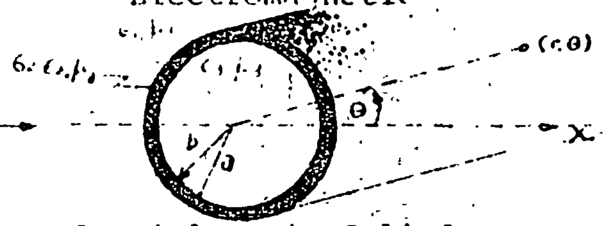	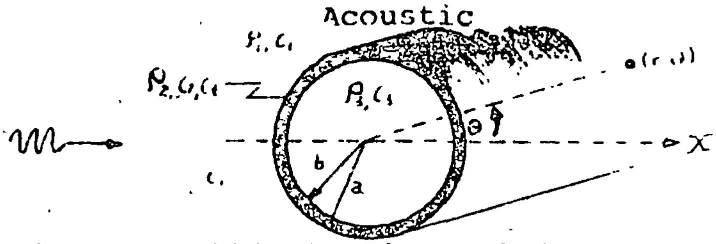
b = 0 Dielectric Cylinder (W. L. Weeks, 1964)	b = 0 Solid Elastic Cylinder (R. D. Doolittle, 1966)
$\sigma \to \infty$ Conducting Cylinder (W. L. Weeks, 1964)	$\mu \to \infty$ Rigid Cylinder
$b \cong a$ Thin Cylindrical Shell	$b = 0,\ \mu = 0,\ \lambda = 0$ Liquid Cylinder (P. Tamarkin, 1949)

$$\Phi_{total} = \Phi_{incident} + \Phi_{scattered}$$

$$\Phi_{incident} = \Phi_o e^{iKx} = \Phi_o \sum_{n=0}^{\infty} i^n \epsilon_n J_n(Kr)\cos(n\Theta)$$

$$\Phi_{scattered} = \Phi_o \sum_{n=0}^{\infty} i^n \epsilon_n a_n H_n^{(1)}(Kr)\cos(n\Theta)$$

where: $\epsilon_n = 2 - \delta_{no} = \begin{cases} 1 & \text{for } n = 0 \\ 2 & \text{for } n \neq 0 \end{cases}$

a_n = constant depending on the boundary conditions

Jn, Hn = Bessel and Hankel functions

$e^{-i\omega t}$ = time dependence has been supressed

Electromagnetic	Acoustic
Φ = E = Electric Potential	Φ = P = Pressure Potential
σ = Conductivity	μ = Lamé Constant
ϵ = Permitivity	ρ = density
μ = Permeability	$C_{l,t}$ = Velocities (Longitudinal, transverse)

(H. Uberal, 1966) **Scattering from Rigid or Conducting Cylinder**

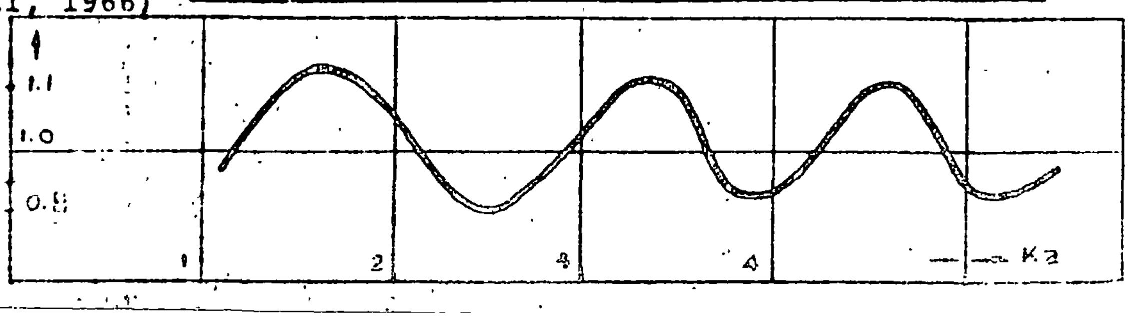

SCATTERING FROM A SPHERE

Electromagnetic	Acoustic

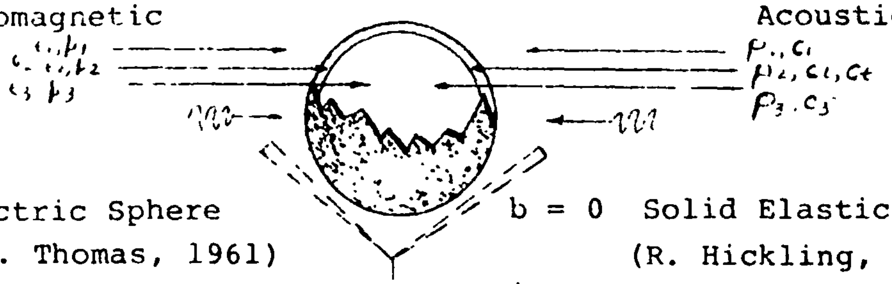

b = 0 Dielectric Sphere (D. T. Thomas, 1961)	b = 0 Solid Elastic Sphere (R. Hickling, 1962)
$\sigma \to \infty$ Conducting Sphere (R. F. Goodrich, 1961)	$\mu \to \infty$ Rigid Sphere (R. B. Lindsay, 1960)
b ≅ a Spherical Shell (A. L. Laden, 1952)	b = 0, μ = 0, $\lambda \neq 0$ Liquid Sphere (A. L. Laden, 1952)

$$\Phi_{total} = \Phi_{incident} + \Phi_{scattered}$$

$$\Phi_{incident} = \Phi_o \exp(iKr\cos\theta) = \Phi_o \sum_{n=0}^{\infty} (2n+1) i^n P_n(\cos\theta) j_n(Kr)$$

$$\Phi_{scattered} = \Phi_o \sum_{n=0}^{\infty} a_n h_n(kr) P_n(\cos\theta)$$

where a_n = constant depending on the boundary conditions

P_n = Legendre polynomial

h_n = spherical Bessel function

J_n = Bessel function

$e^{-i\omega t}$ = time dependence has been supressed

$\Phi = E$ = Electric Potential	$\Phi = P$ = Pressure
σ = Conductivity	μ = Lamé Const.
ϵ = Permitivity	ρ = Density
μ = Permeability	$C_{l,t}$ = Velocities of Sound

Scattering from Rigid or Conducting Sphere (R. F. Goodrich, 1961

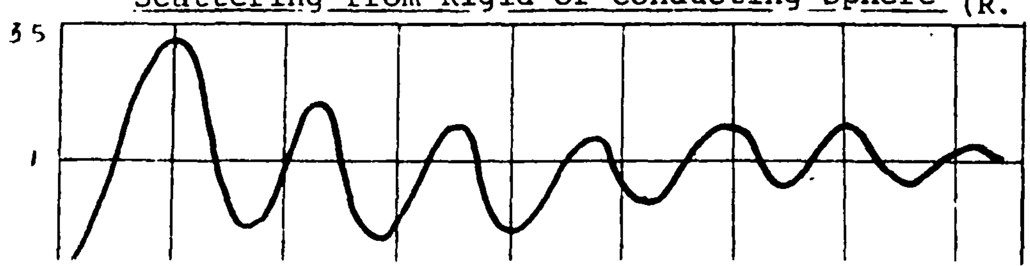

SCATTERING FROM A CONE

Electromagnetic   Acoustic

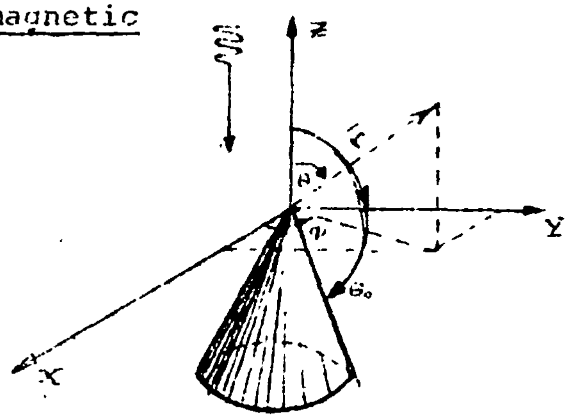

$x = r \cos\phi \sin\theta$

$y = r \sin\phi \sin\theta$

$z = r \cos\theta$

For the special case of a finite cone, flat-backed (base is circular or radius a), and a given height h with a semivertex angle $\pi - \theta_0$ the scattered far field amplitude is given by the following approximation formula (good for high frequencies). (R. F. Kleinman 1966)

$$S = \frac{4i\pi}{\lambda^2} \tan^2\theta_0 \int_0^h e^{2iKu} du$$

Flat-backed cone $\pi - \theta_0 = 4°$ (R. F. Kleinman, 1966)

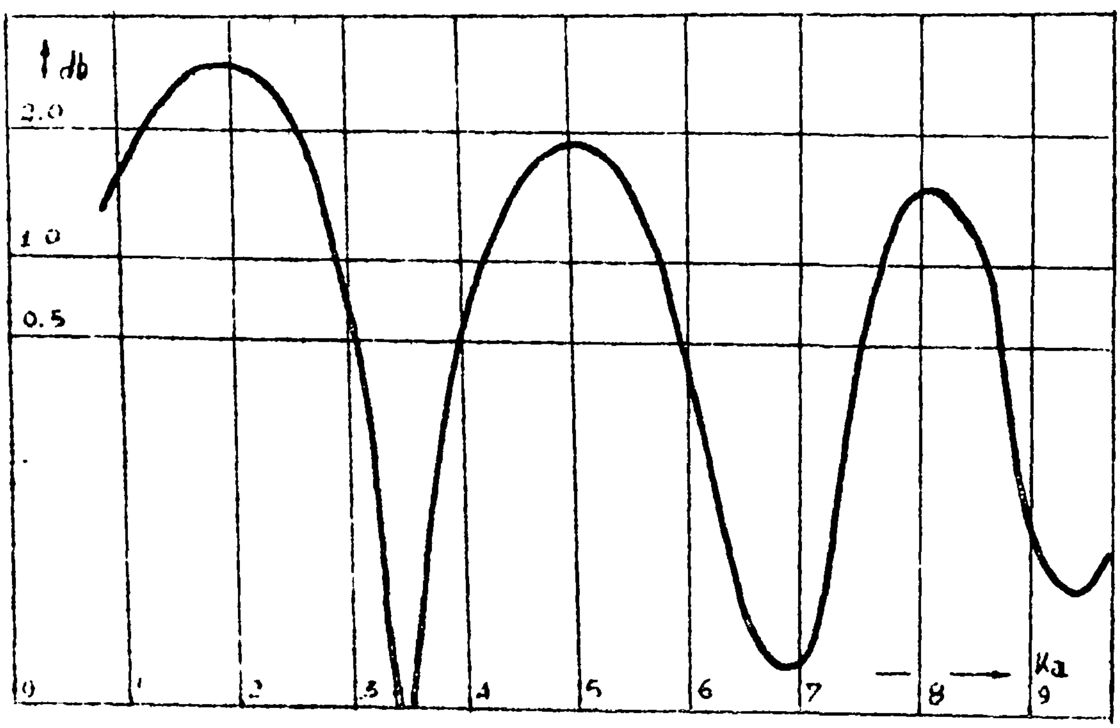

Experimental Verification. *

For *nearly* smooth surfaces, the surface characteristic constant $1/B \to 0$, and (3.15) gives the scattering coefficient. This result compares very closely with published results [Nielson, 1960] for new ice as shown in table 2.

For rough (not *nearly* smooth) surfaces, (3.14) describes the relationship of the scattering coefficient σ_0 and other variables such as the angle of incidence θ, wavelength λ, standard deviation σ and surface covariance constant B, etc. Two curves of the scattering coefficient σ_0 versus θ for each of the three values of λ/B, 0.1, 0.5, and 1.0 for σ/λ equal to 0.05, and 0.1 are shown in figure 4. It may be noticed that as the surface becomes rougher, or as λ/B increases for a specified λ, the scattering coefficient curve becomes flatter, showing the relative importance of the contribution of the power return from the surface at angles other than those near zero. As expected, when the surface becomes smoother or $1/B$ decreases, the received power seems to come primarily from near-zero angles. These curves are quite similar to those recently published [Campbell, 1959; Dye, 1959; Edison, 1960]. The experimental data [Nielson, 1960] on desert and new ice also seems to follow the pattern of these theoretical curves described above.

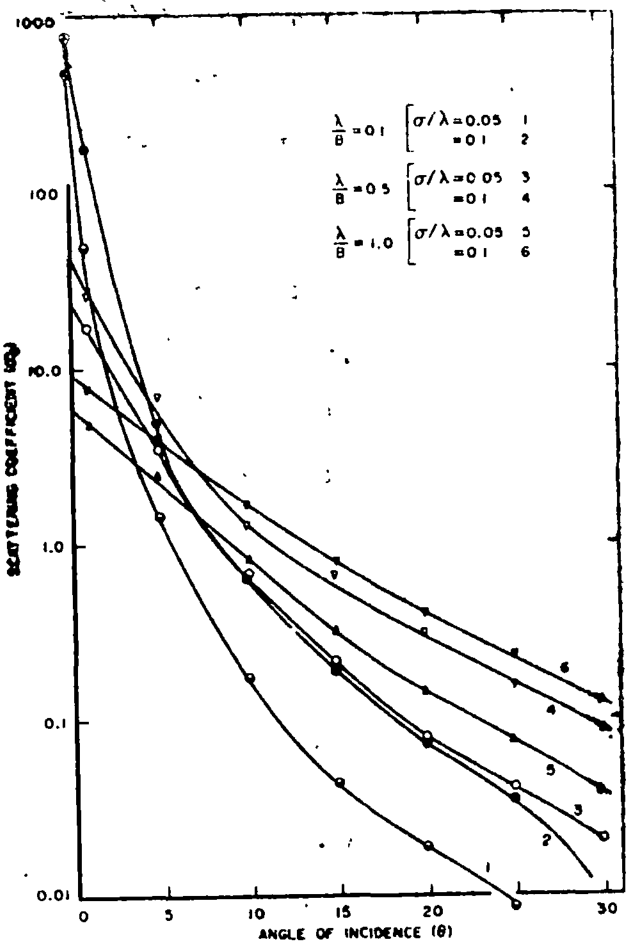

FIGURE 4. *Scattering coefficient versus the angle of incidence.*

The scattering coefficient (σ_0) for nearly smooth surfaces is inversely proportional to the wavelength, but varies directly with (σ^2), ($\theta \cot^4 \theta$) and $1/B$, where σ, θ, B are standard deviation, angle of incidence, and the terrain characteristic constant respectively. For rough surfaces it has a negative exponential factor, where the exponent is made up of $\frac{\sigma^2 \cos^2 \theta}{\lambda^2}$ times a constant. The surface characteristic constants B and σ can be calculated from the radar return data. Although approximate, the theoretical results agree well with the experimental data; and therefore, suggest the usefulness of the approach. The application of these results may be extended to the moon-echo data, with proper corrections for Faraday and liberation effects, etc. This investigation has established that for near-vertical incidence, the normalized autocovariance for the terrain elevation is more often of the exponential form $\exp(-|r|/B)$ rather than the Gaussian form, $\exp(-r^2/B)$. The former may well be more appropriate for finer terrain irregularities than those considered in this

Comparison of theoretical versus experimental scattering coefficient

(Normalized)

θ^0	σ_0 Theoretical	σ_0 Experimental
30	1.000	1.000
40	0.291	0.308
50	.088	.089
60	.022	[illegible]
70	.004	.004

* H S HAYRE & R.K. MOORE. Theoretical Scattering Coef for near Vertical Incidence From Contour Maps, Journal of Research Vol. 65D, Sept-1961 pp 431.

The distinction between beam-width and pulse-length limiting of the illuminated area is a function of altitude[1] and is given by

$$1 + \frac{v\tau}{2h} = \sec \theta_0 \quad (6\text{-}1)$$

where

v is the velocity of propagation,

τ is the pulse width,

h is the altitude, and

θ_0 is the effective half-angle of the antenna pattern.

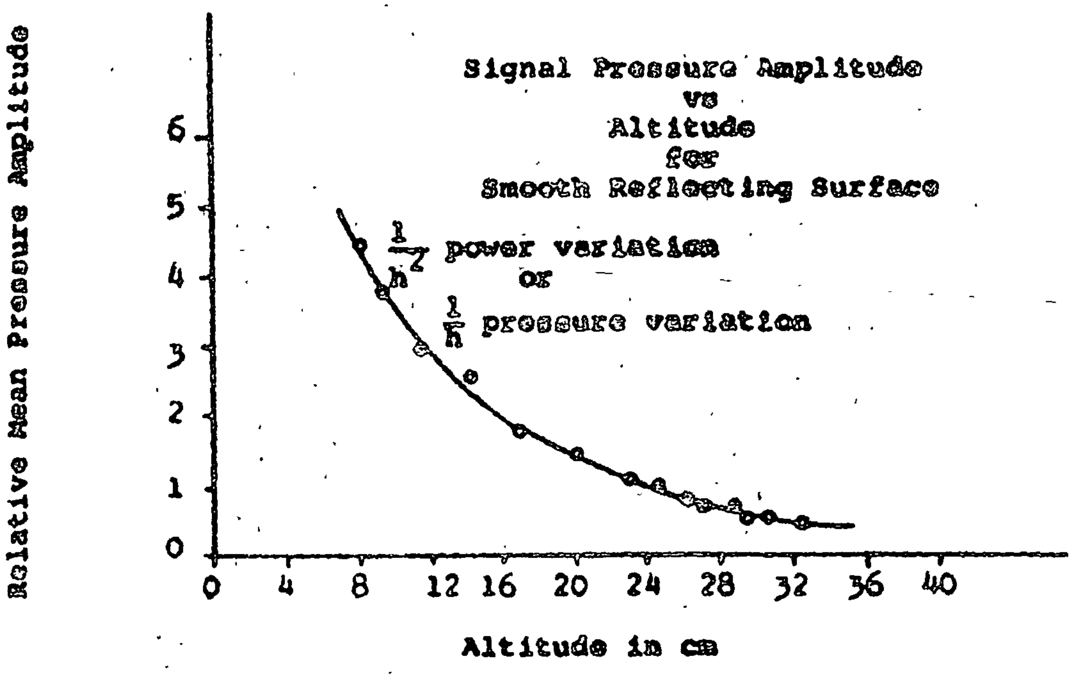

Signal vs Altitide over Smooth Surface (EDISON, 1961)

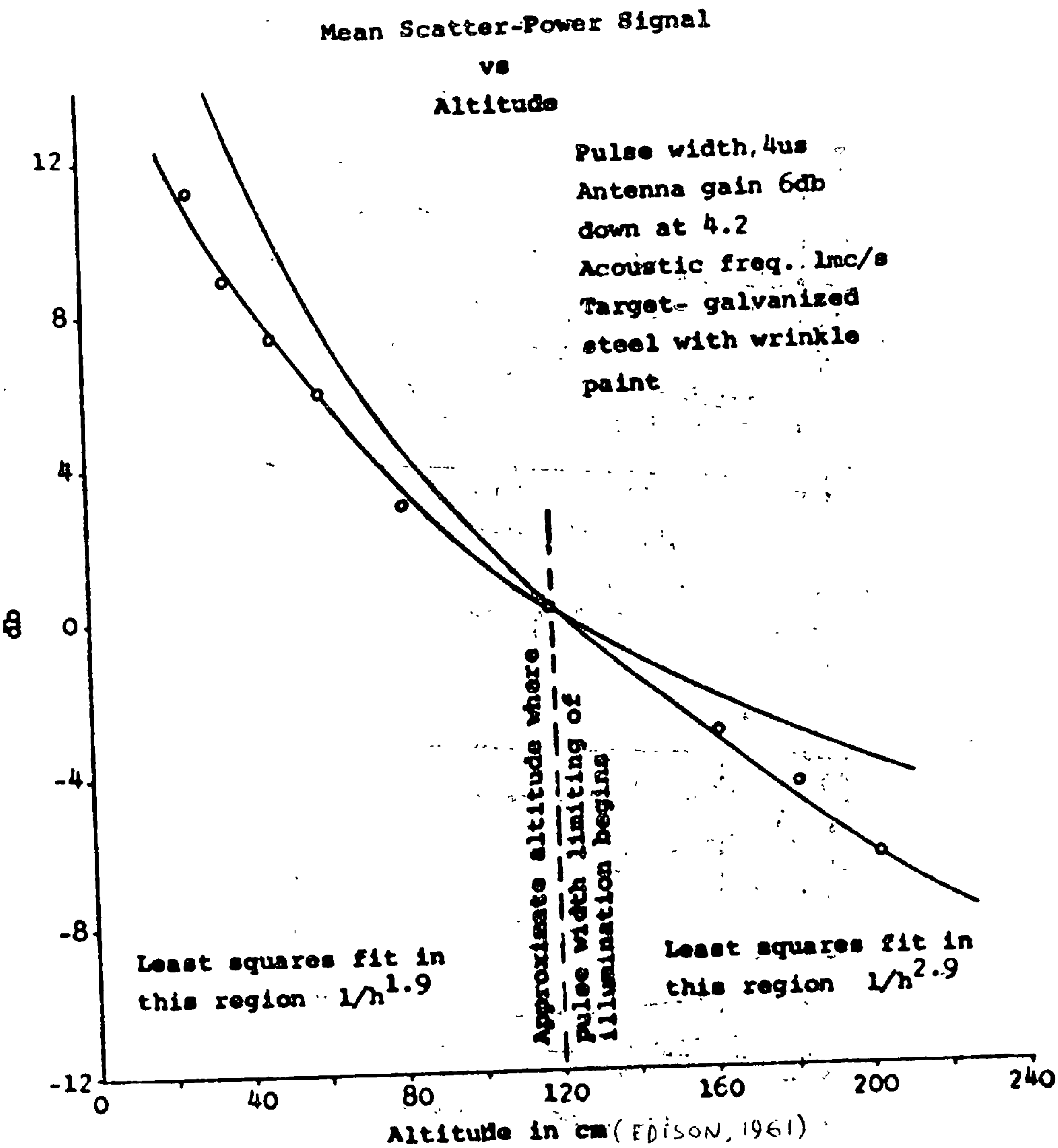
Mean Scatter-Power Signal
vs
Altitude
Pulse width, 4us
Antenna gain 6db
down at 4.2
Acoustic freq. 1mc/s
Target- galvanized
steel with wrinkle
paint
12
8
4
0
-4
-8
-12
db
Least squares fit in
this region 1/h1.9
Approximate altitude where
Pulse width limiting of
illumination begins
Least squares fit in
this region 1/h2.9
0
40
80
120
160
200
240
Altitude in cm (EDISON, 1961)

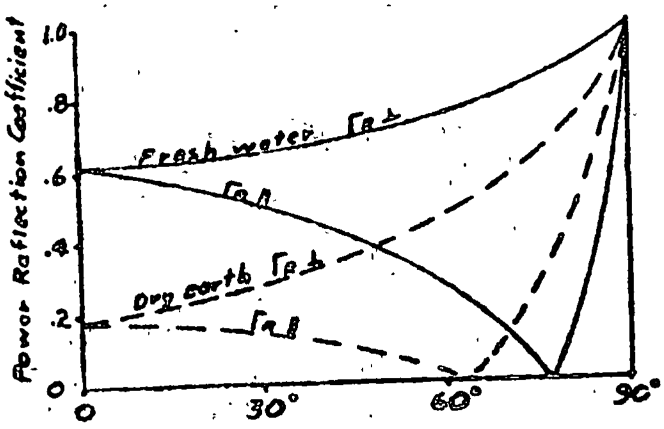

Angle of Incidence

Reflection Coefficients for TM and TE Waves
Figure 3-8

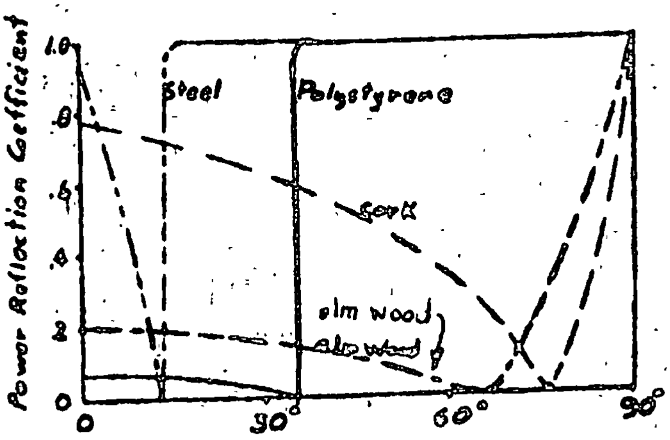

Angle of Incidence

Reflection Coefficient for Acoustic Waves (EDISON, 1961)

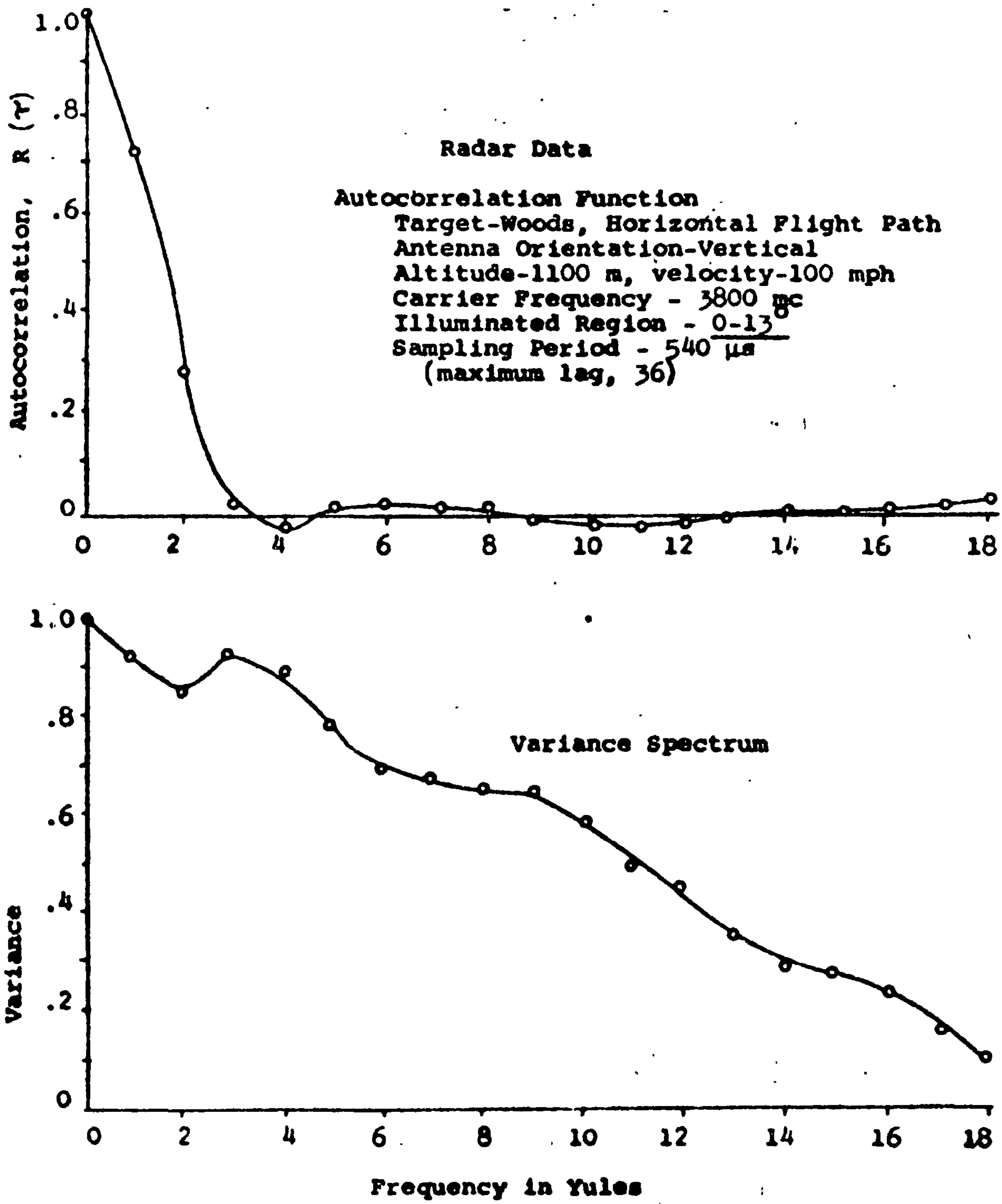

Variance Spectrum for Wooded Terrain (EDISON, 1961)

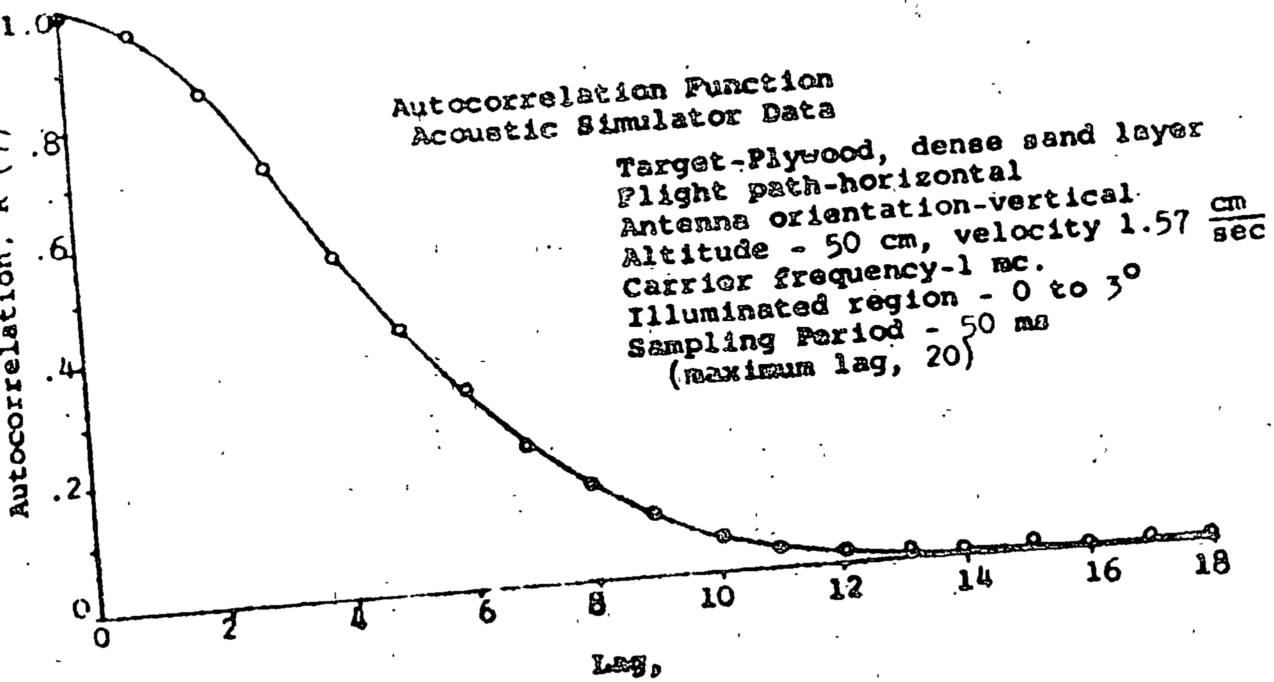

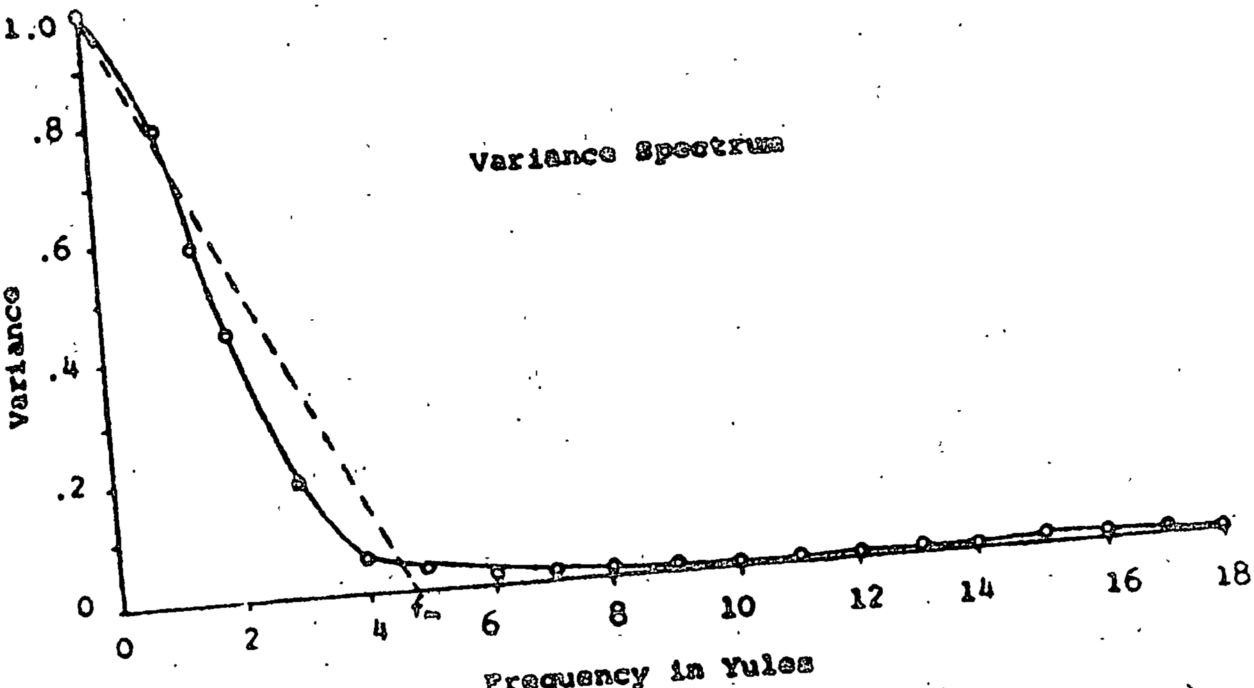

Variance Spectrum for Rough Sand (EDISON, 1961)

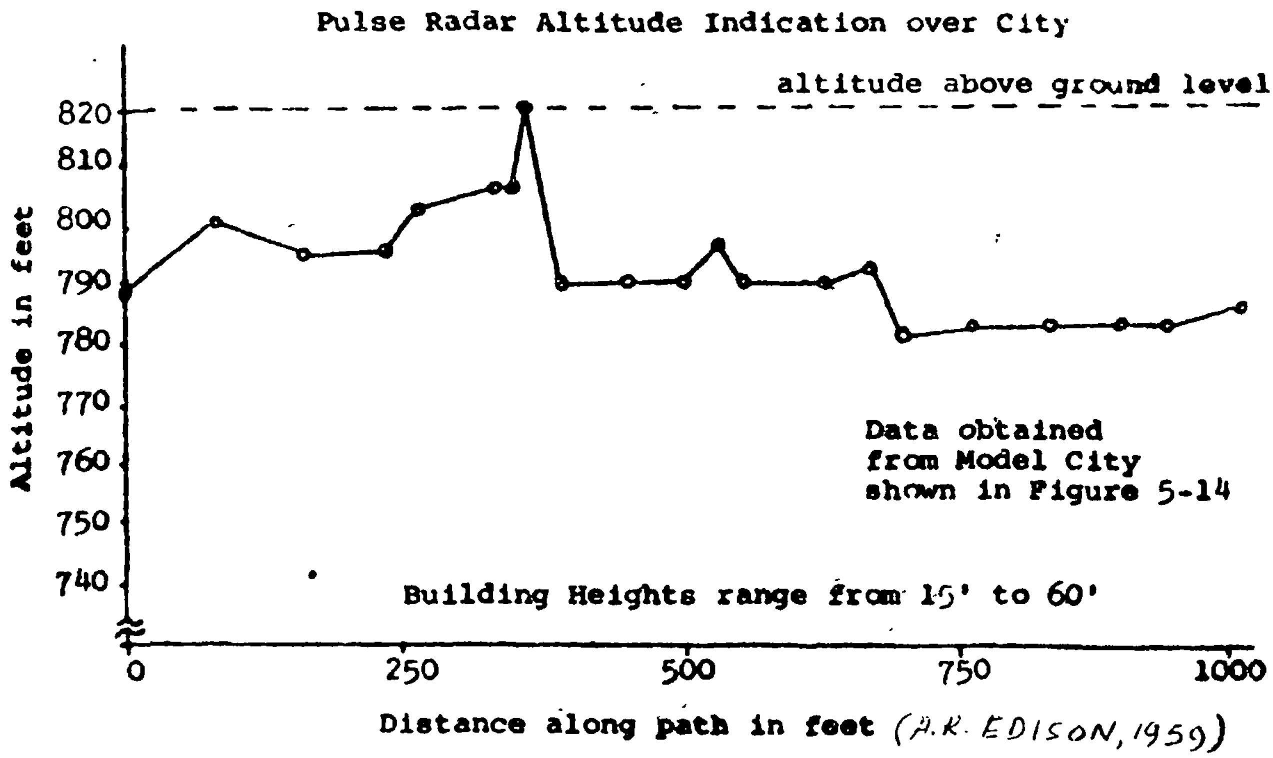

Pulse Radar Altitude Indication over City
altitude above ground level
Altitude in feet
820
810
800
790
780
770
760
750
740
Data obtained from Model City shown in Figure 5-14
Building Heights range from 15' to 60'
0
250
500
750
1000
Distance along path in feet (A.R. EDISON, 1959)

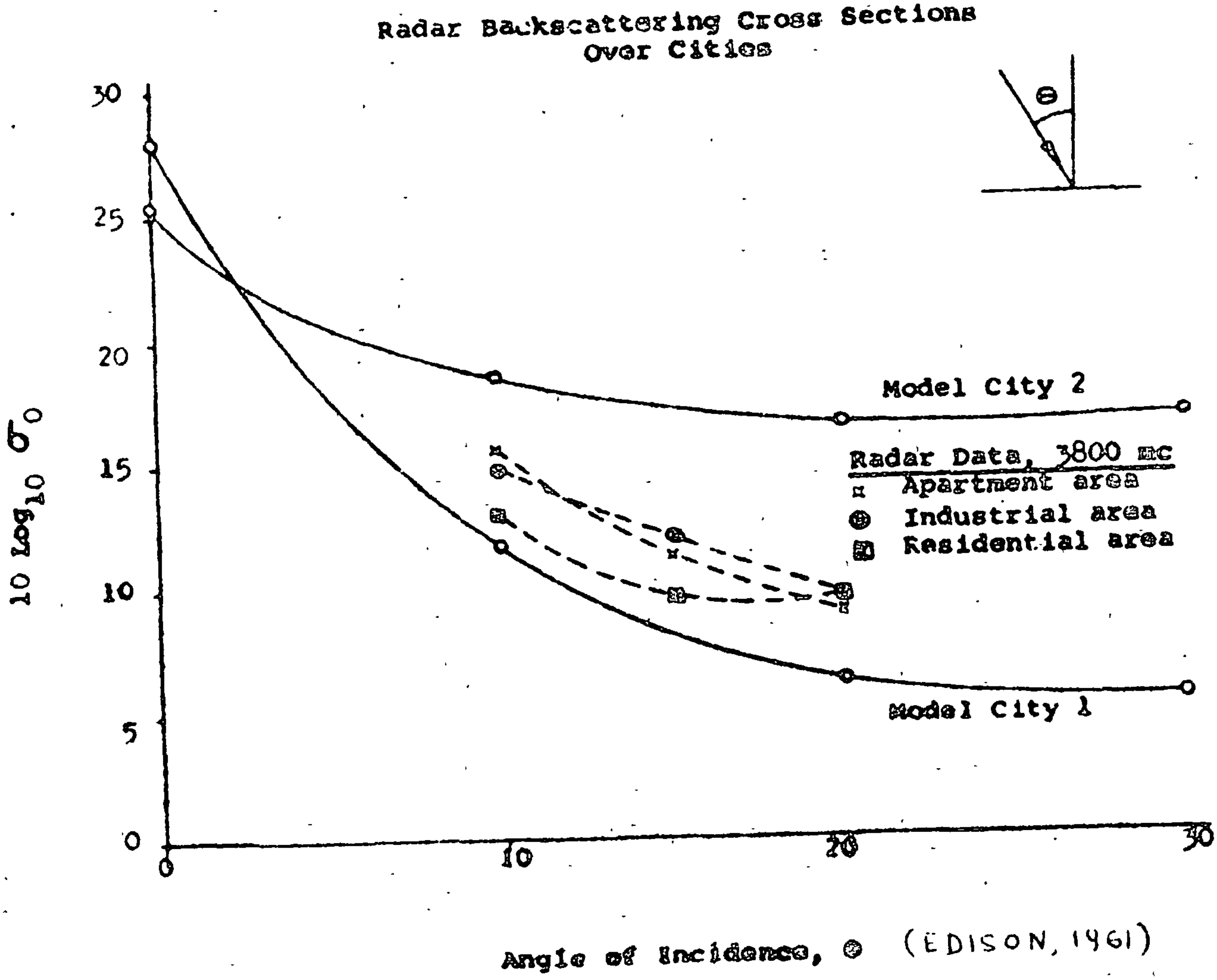

Radar Backscattering Cross Sections
Over Cities
30
25
20
15
10
5
0
10 Log10 σ0
θ
Model City 2
Radar Data, 3800 mc
Apartment area
Industrial area
Residential area
Model City 1
0
10
20
30
Angle of Incidence, θ
(EDISON, 1961)

TARGET RECOMMENDATIONS (EDISON 1961)

Terrain	Target Base	Sand Particle size, wavelengths	Distance Between Particles, Wavelengths
Woods	Plywood	1-2	0 - 1/2
Farmland	"	1-2	1 - 5
Desert	"	---	-----
Cities	" (buildings)[a]	$\frac{1}{2}$-1	1 - 5
Water (smooth)	galv. steel	< $\frac{1}{2}$	3 - 5
Water (rough)	" "	$\frac{1}{2}$-1	1 - 2
Mountains	" " (shaped)[b]	$\frac{1}{2}$-1	1 - 2

[a]Buildings are pine blocks cut to size.

[b]Steel can be formed into appropriate contours.

It should be observed that the slope of the radar backscattering cross section curves is important in modeling practice. The absolute level of the curves can be increased or decreased by proper scaling.

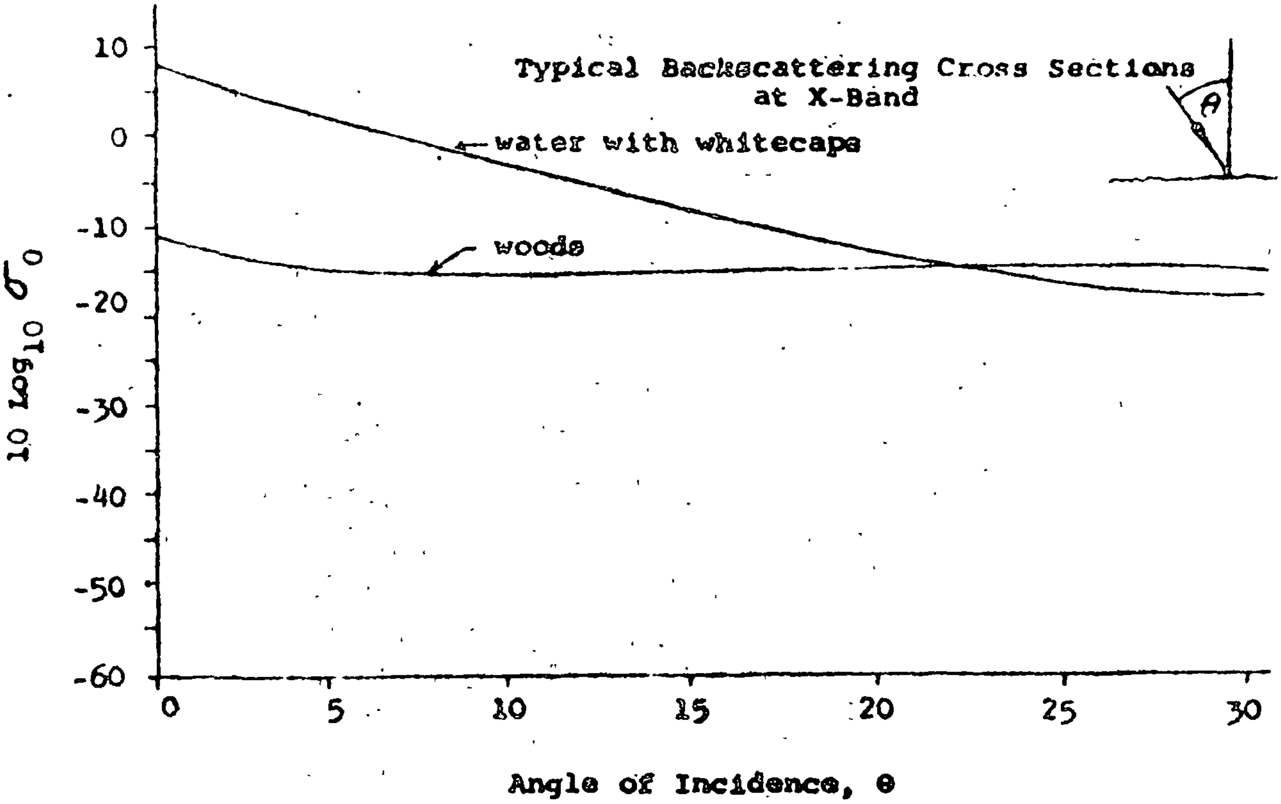

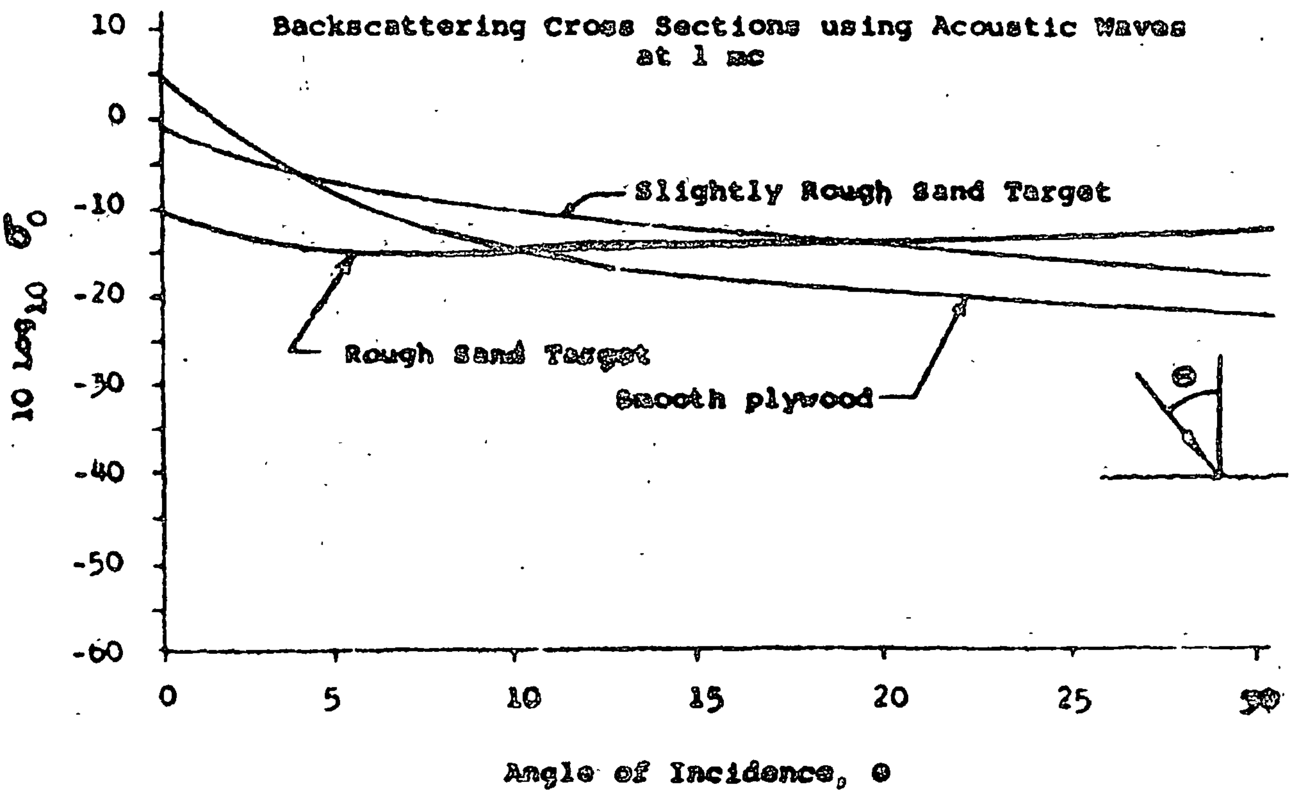

Typical Radar Back-Scattering Cross Sections (EDISON, 1961)

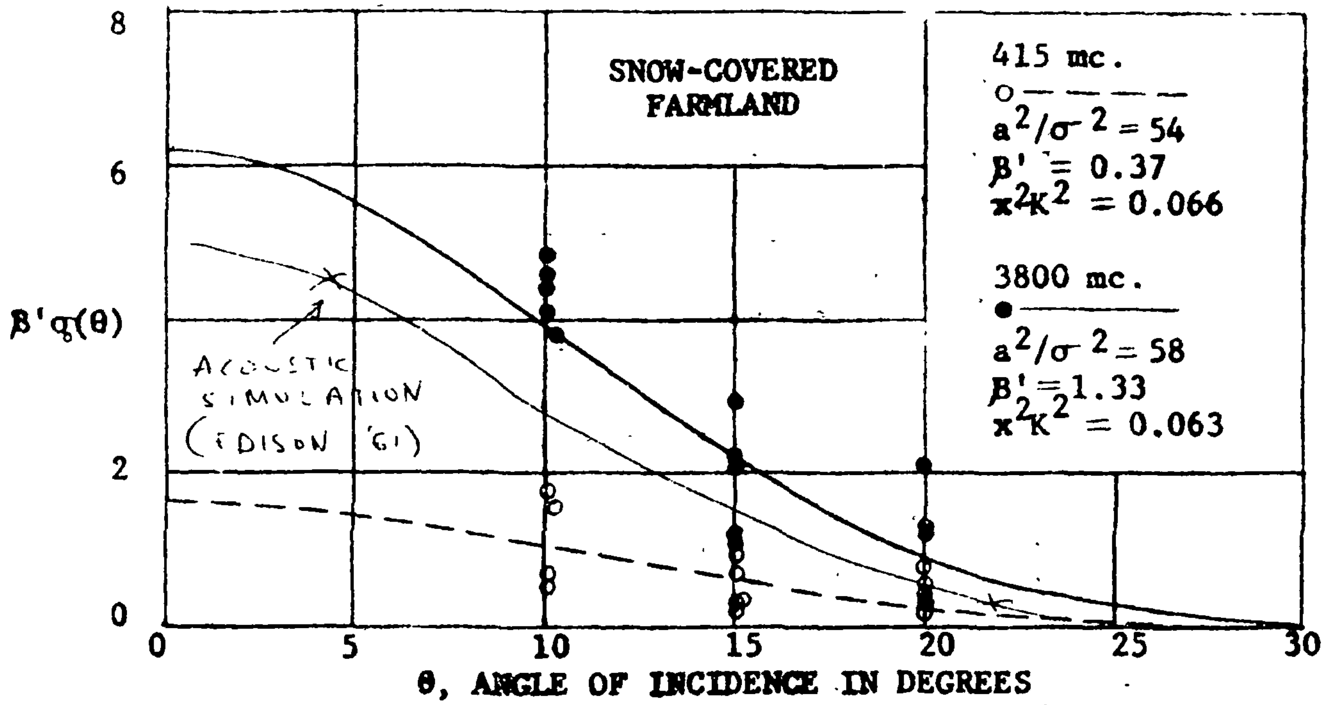

Median scattering curves for snow-covered farmland near Wahpeton, North Dakota. The target area was flat crop land containing two dry stream beds and was covered by eight inches of dry snow. (EDISON, '59)

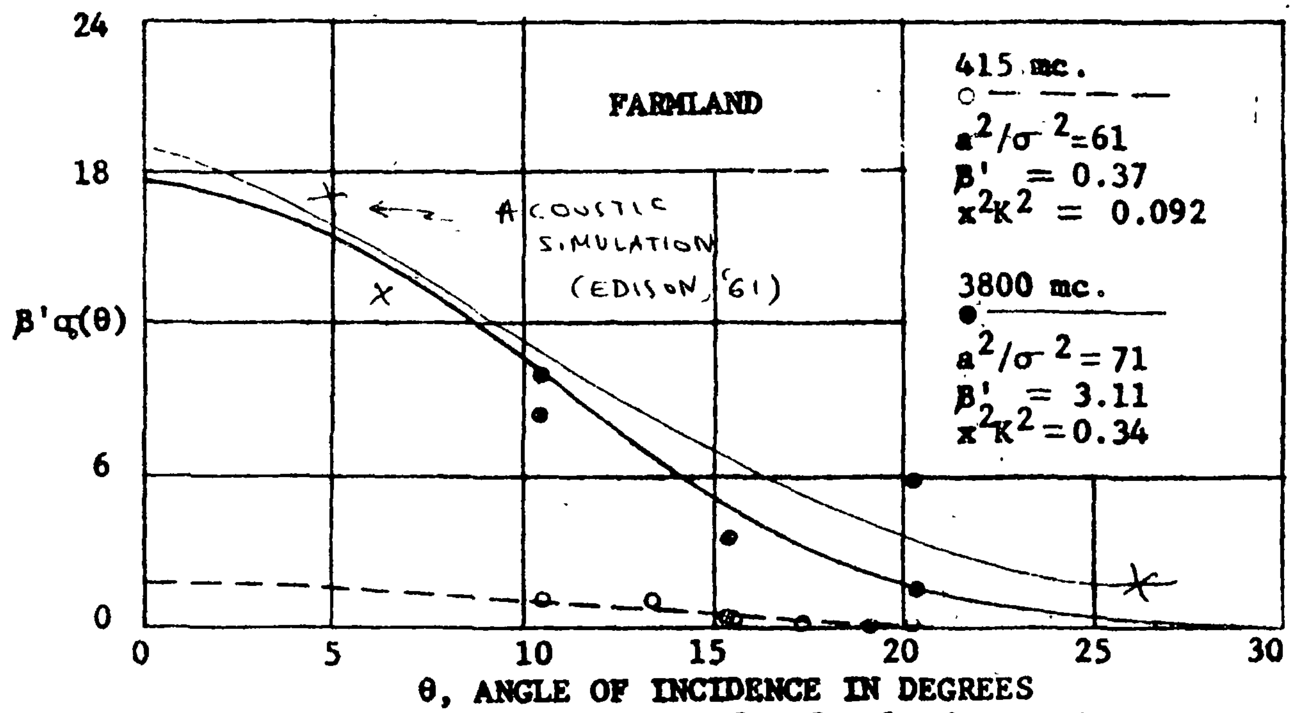

Median scattering curves for farmland near Cameron, Missouri. The target area was flat pasture and crop land containing a single line railroad. (EDISON, '59)

7.0a Scattering Cross Sections

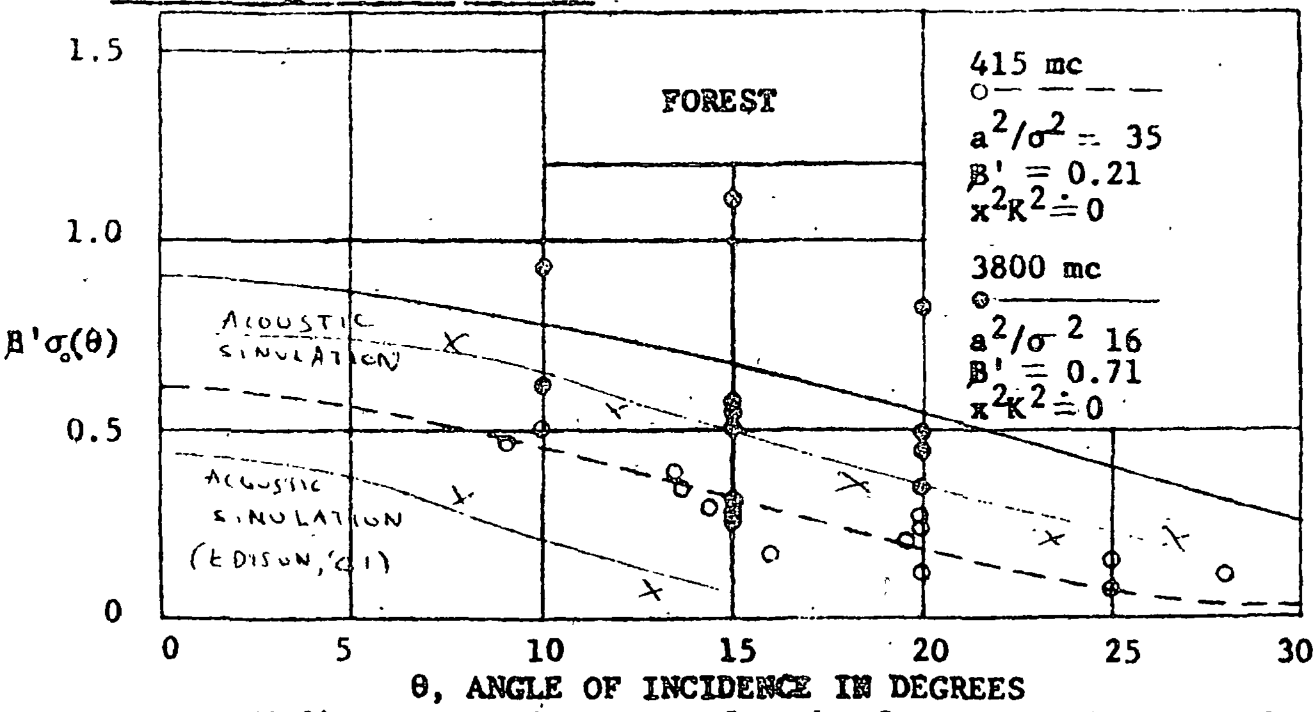

Median scattering curves for the forest at Pine Island, Minnesota. The target area was very flat and densely covered with pine, hemlock, birch, white ash, and elm trees from 20 to 40 feet in height.

(EDISON '59)

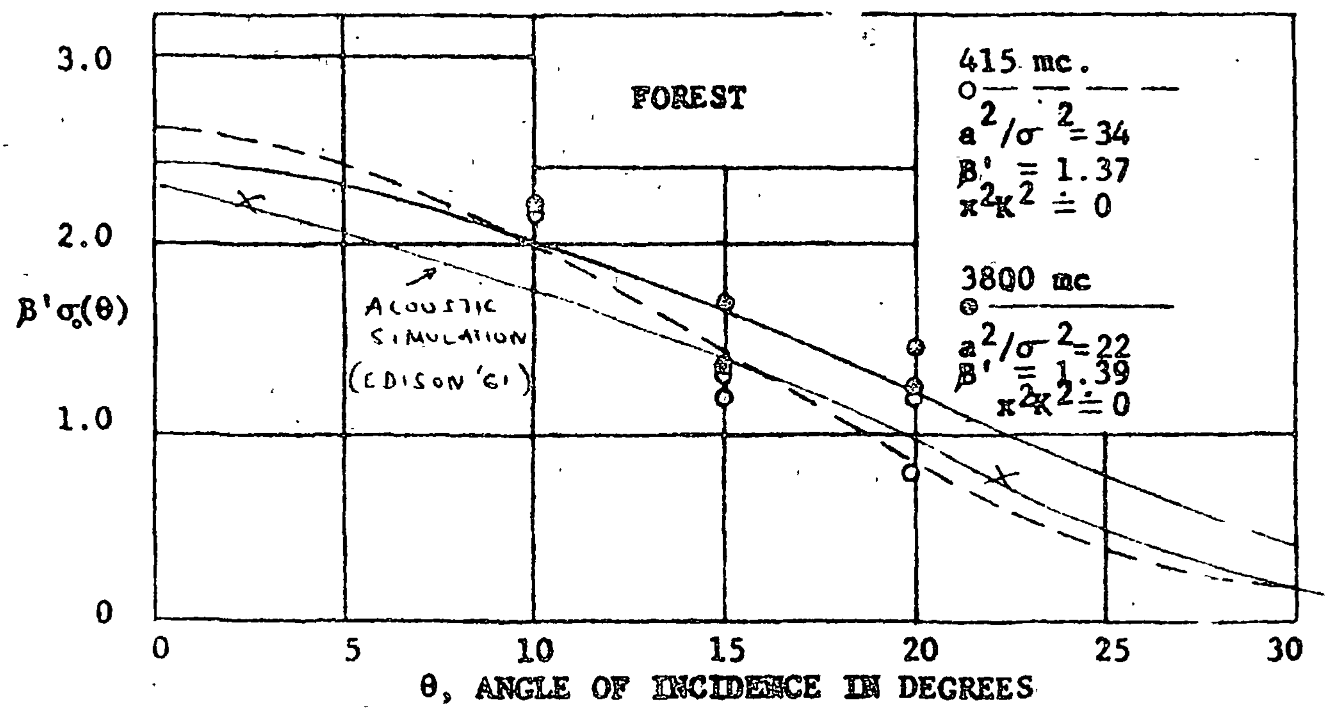

Median scattering curves for the forest at Presque Isle, Maine. The target had a snow-and-ice-covered rolling surface with a homogeneous covering of snow-bare evergreen fir and pine trees from 20 to 50 feet in height.

(EDISON '59)

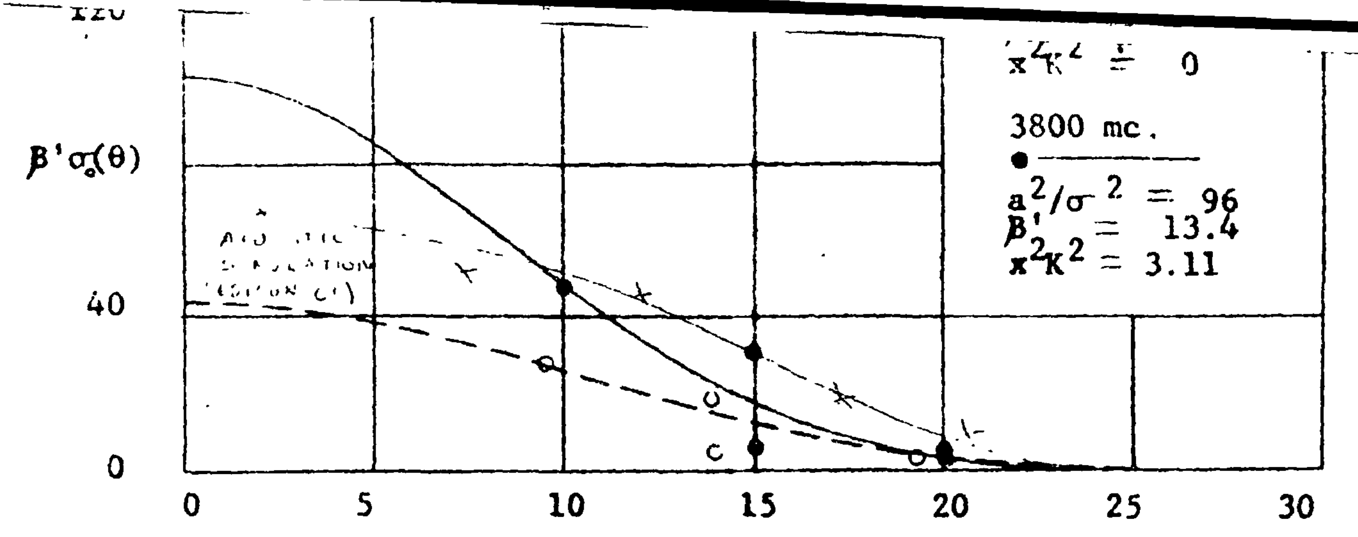

Median scattering curves for a moderately rough surface on Lake Bemidji, Minnesota. The ripples and swells were about 15 to 20 inches vertically from peak to trough and three to four feet horizontally from peak to peak.
(EDISON,'59)

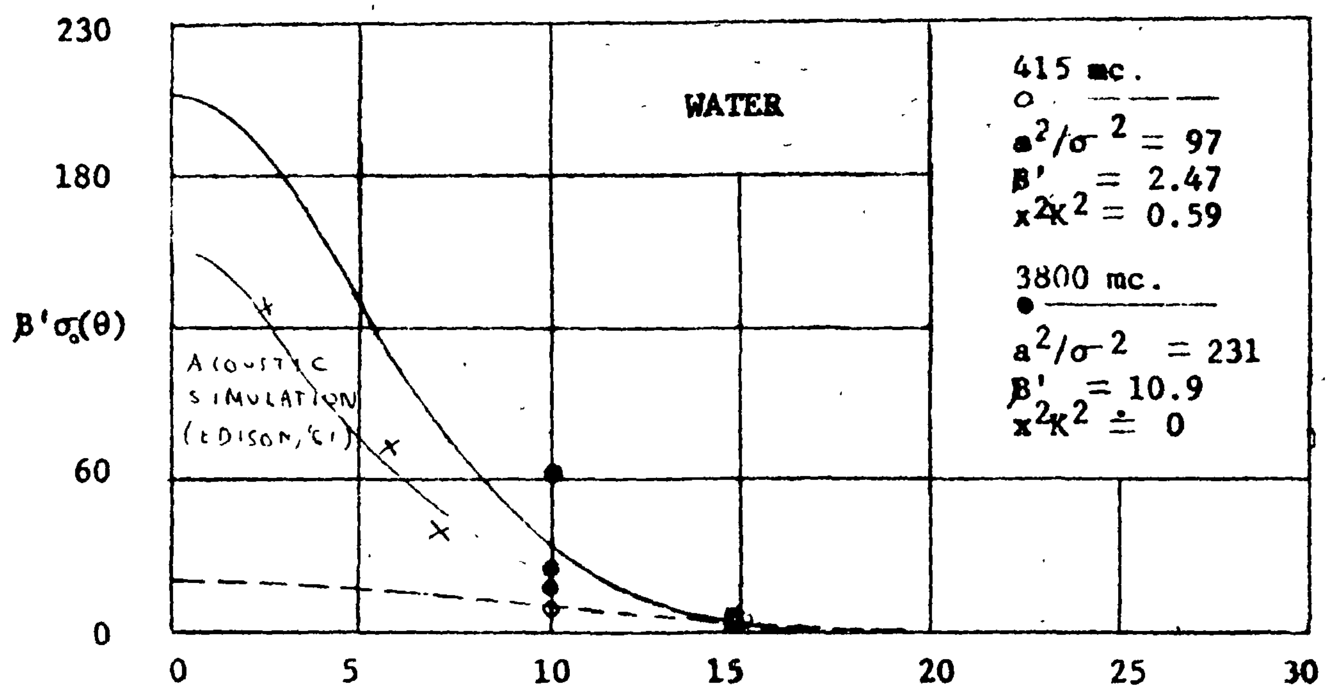

Median scattering curves for a relatively smooth surface on the Salton Sea in California. The air over the target was quite calm at the time of the flights.
(EDISON,'59)

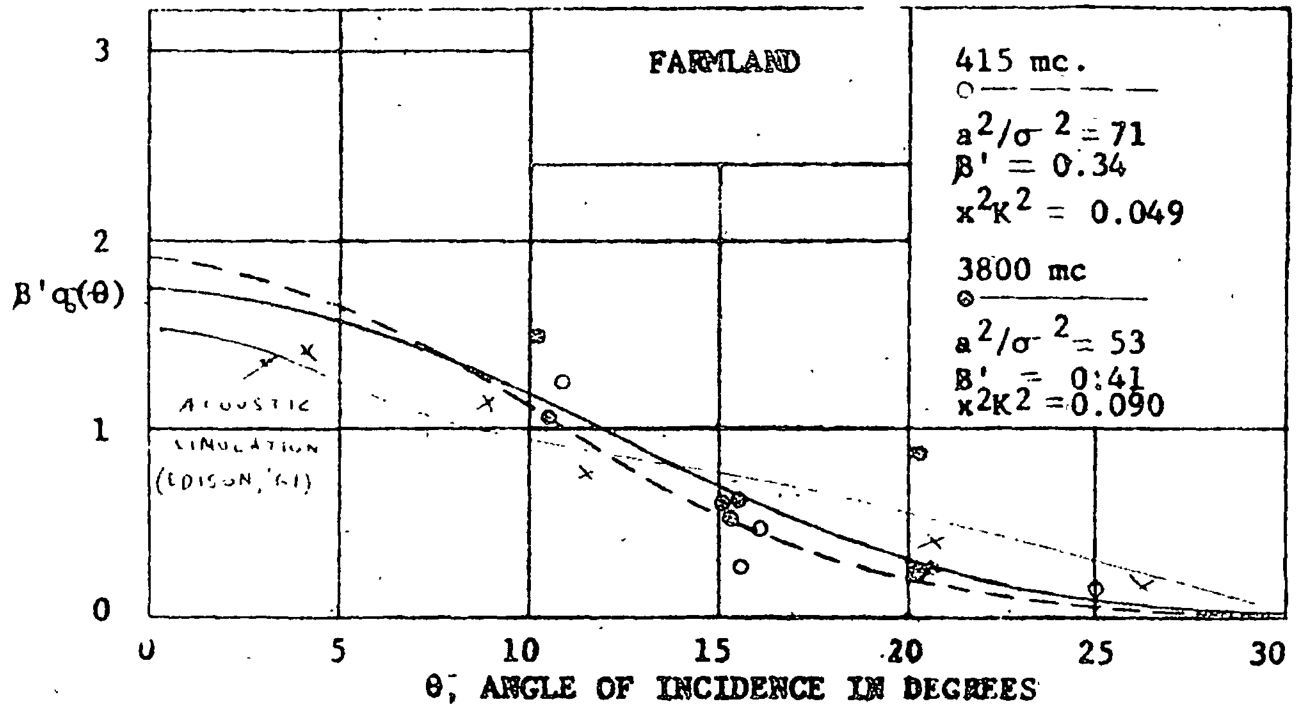

. Median scattering curves for farmland near Sioux City, Iowa. The target area was flat crop land which had recently been plowed. (EDISON, '59)

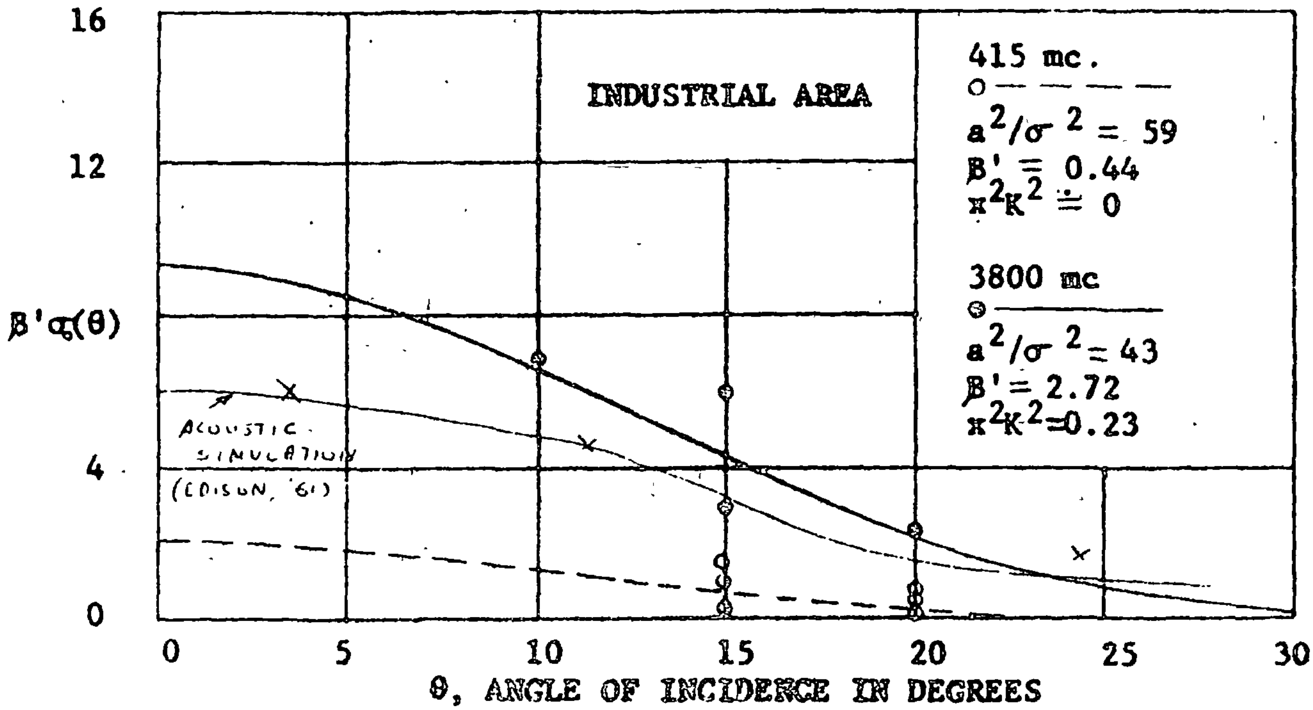

..Median scattering curves for industrial area in Minneapolis, Minnesota. The target contained a predominant number of metal roofed factory buildings with a railroad yard at one edge. (EDISON, '59)

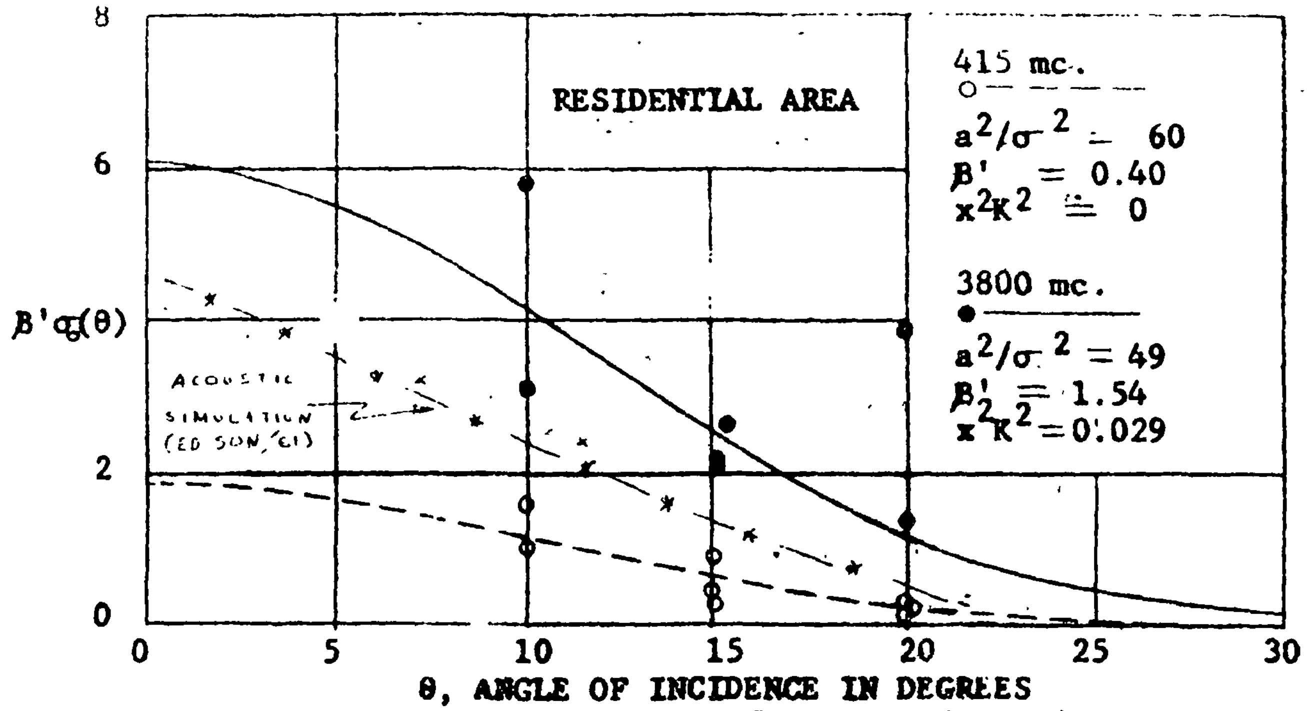

. Median scattering curves for a residential area in Minneapolis, Minnesota. The target area was built up of one and two story brick and frame houses with pitched roofs, and had many old, well established trees. (EDISON, 1959)

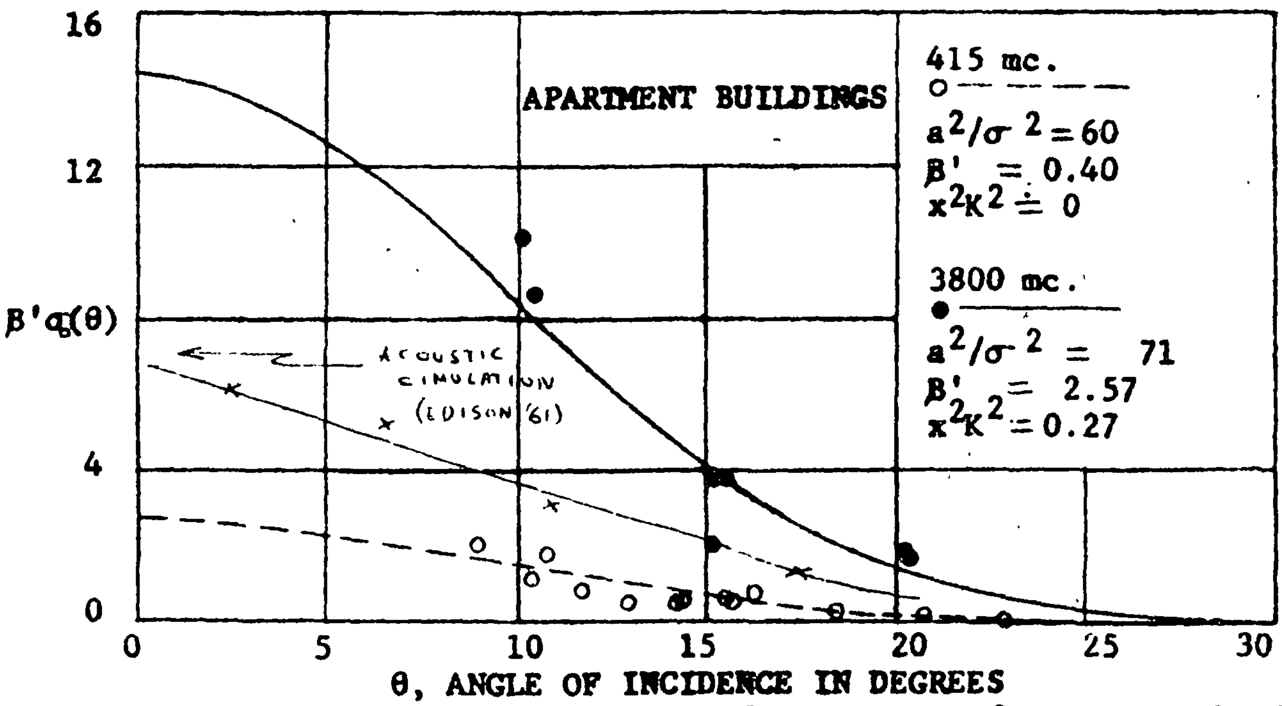

. Median scattering curves for an area of apartment buildings in Kansas City, Missouri. The majority of the buildings were built of brick, flat roofed, and several stories tall. (EDISON, 1959)

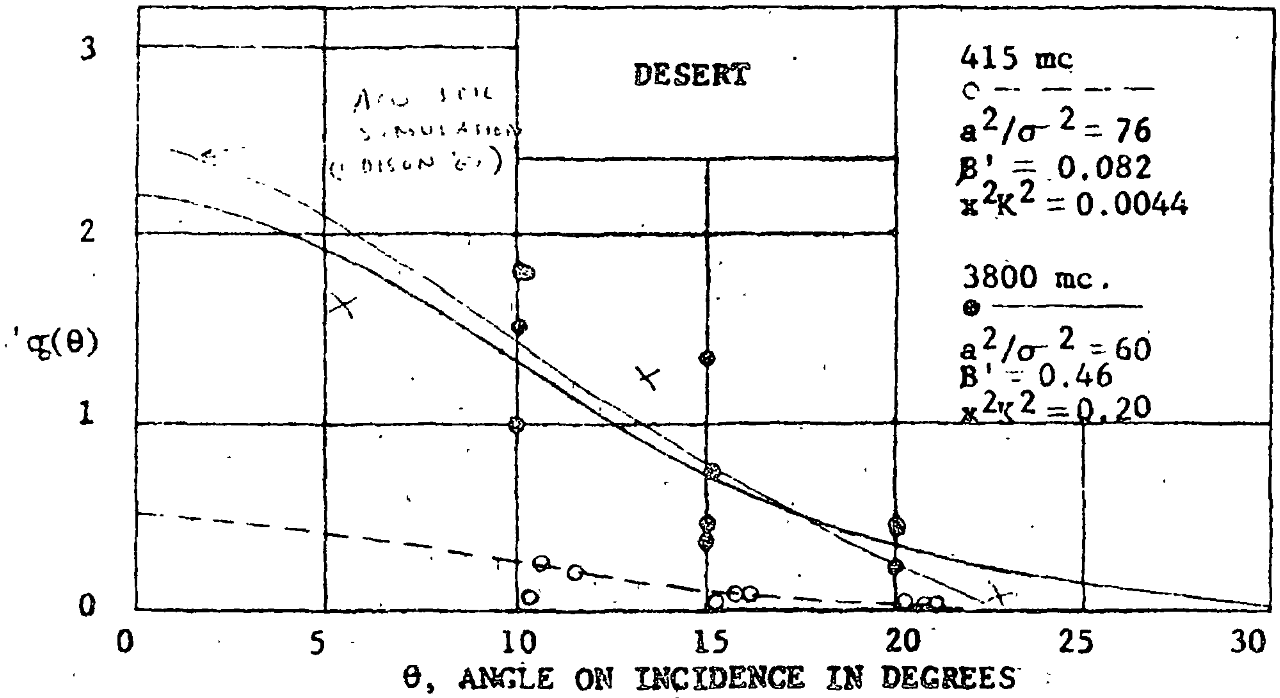

Median scattering curves for a desert area near Salton Sea, California. The target area was flat, arid, sandy, and barren. (EDISON '59)

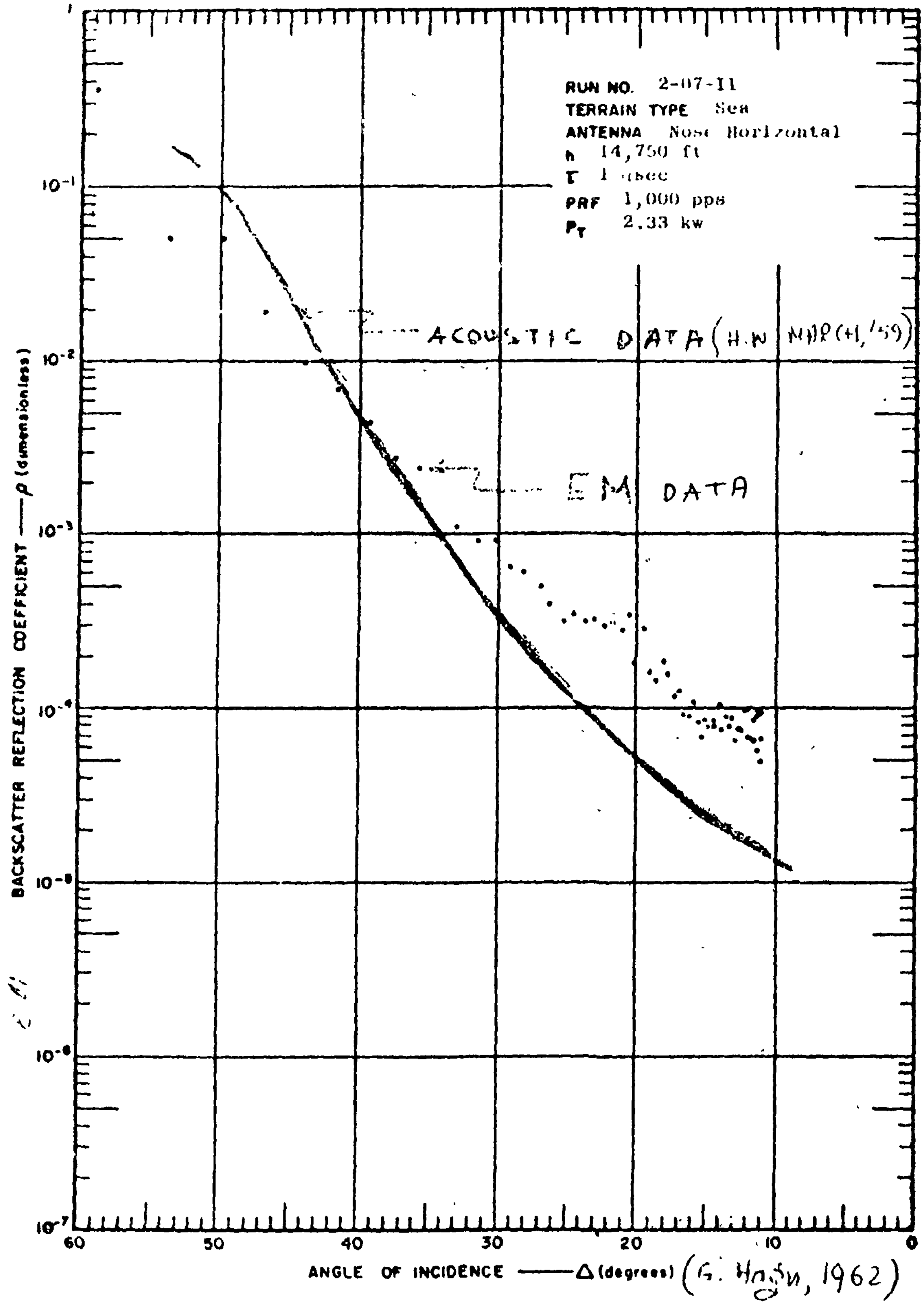

RUN NO. 2-07-I1
TERRAIN TYPE Sea
ANTENNA Nose Horizontal
h 14,750 ft
τ 1 μsec
PRF 1,000 pps
P_T 2.33 kw
ACOUSTIC DATA (H.W. N...)
EM DATA
BACKSCATTER REFLECTION COEFFICIENT — ρ (dimensionless)
ANGLE OF INCIDENCE — Δ (degrees)
(G. Hagn, 1962)

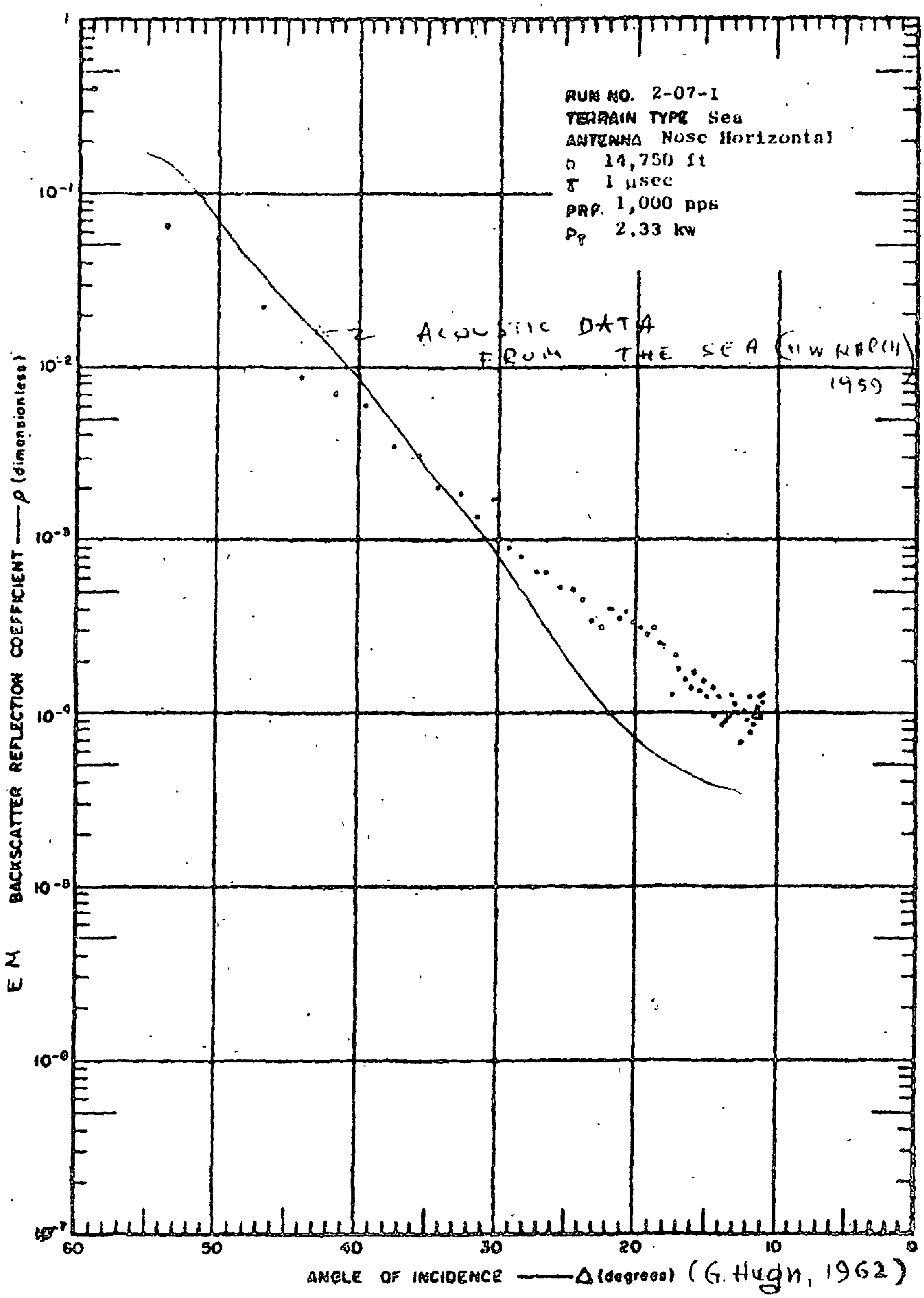
RUN NO. 2-07-1
TERRAIN TYPE Sea
ANTENNA Nose Horizontal
h 14,750 ft
τ 1 µsec
PRF 1,000 pps
Pt 2.33 kw
ACOUSTIC DATA FROM THE SEA
1959
1
10⁻¹
10⁻²
10⁻³
10⁻⁴
10⁻⁵
10⁻⁶
10⁻⁷
EM BACKSCATTER REFLECTION COEFFICIENT — ρ (dimensionless)
60
50
40
30
20
10
0
ANGLE OF INCIDENCE — Δ (degrees)
(G. Hugn, 1962)

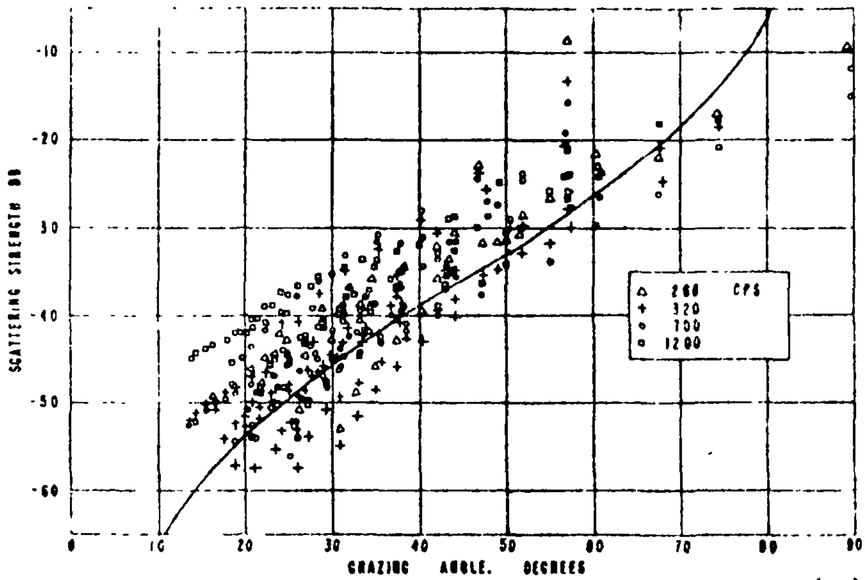

Scattering strength vs grazing angle. (H W March, '63)

ACOUSTIC SCATTERING FROM THE SEA

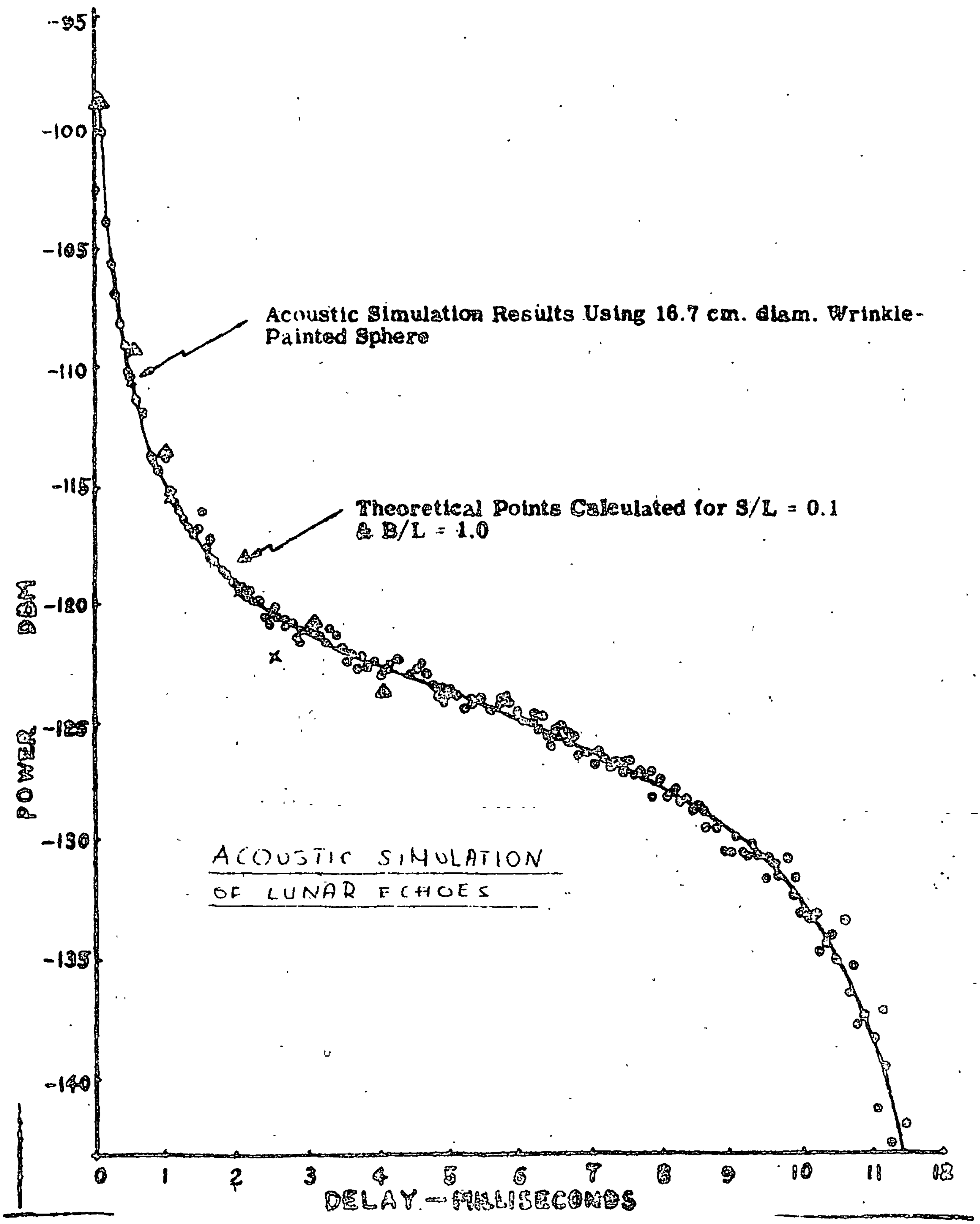

Hayre, H. S. "Acoustic Simulations of Lunar Echoes," Journal of Geophysical Research, Vol. 70, No. 16, (August, 1965), pp. 3831-3839.

REFERENCES

Abramowitz, W., A. Crews, and R. Erath. Ocean Surface Reverberation: Surface Interface Scattering. Grumman Research Department, May, 1966, Report No. RE-252.

Bechtel, M. E. Scattering Coefficients for the Backscattering of E. M. Waves from Perfectly Conducting Spheres. Cornell Aeronautical Laboratory, Inc., Buffalo 21, New York, December, 1962, pp. 7-11.

Doolittle, R. D. and H. Uberall. Journal of Acoustical Society of America, Vol. 39, 1966, pp. 272-275.

Edison, A. R. An Acoustic Simulation for Modeling Backscatter of Electromagnetic Waves. September, 1961, Technical Report EE-62.

Edison, A. R., R. K. Moore, and B. D. Warner. Radar Return at Near-Vertical Incidence. September, 1959, Technical Report EE-24.

Goodrich, R. F., B. A. Harrison, R. E. Kleimnan, and T.B.A. Senior. Diffraction and Scattering from a Sphere. Air Force Cambridge Research Laboratory, Bedford, Massachusetts, December, 1961, Report 3648-1-T.

Hagn, George. An Investigation of the Direct Backscatter of High Frequency Radio Waves from Land, Sea Water, and Ice Surfaces. (1962) STANFORD RESEARCH INSTITUTE, CALIFORNIA

Harrison, C. W., Jr., and R. O. Heinz. On Radar Cross Section of Rods, Tubes, and Strips of Finite Conductivity. Scandia Corporation...Monograph, July, 1963.

Hickling, Robert. An Analysis of Echoes from a Solid Elastic Sphere in Water. California Institute of Technology, Technical Report No. 85-20, March, 1962.

Kleinman, R. E. and T. B. A. Senior. Diffraction and Scattering from a Cone. Air Force Cambridge Research Laboratory, Bedford, Massachussetts, January, 1963, Report 3648-2-T.

Lindsay, R. B. Mechanical Radiation, McGraw-Hill Book Company, New York, 1960, pp. 101-105.

Lorden, A. L. Backscattering of E. M. Waves from Spheres and Spherical Shells. Air Force Cambridge Research Center, Cambridge, Massachussetts, 1962, Technical Report No. 15, pg. 36.

Marsh, H. W. "Sound Reflection and Scattering from the Sea Surface". Journal of the Acoustical Society of America, Vol. 35, No. 2. (1963)

Tauconkin, P. Journal of Acoustic Society of America, Vol. 21, 1949, pp. 612-616.

Thomas, D. T. Approximation for Backscatter from Dielectric Sphere. Antenna Laboratory, Ohio State University, Report 1116-14, October, 1961.

Uberal, H., R. D. Doolittle, and J. V. McNicholas. "Use of Sound Pulses for a Study of Circumferential Waves", Journal of Acoustical Society of America, Vol. 39, No. 3, 1966, pg. 576.

Ugincius, Peter. Creeping Wave Analysis of Acoustic Scattering by Elastic Cylindrical Shells. U. S. Naval Weapons Laboratory, Dahlgteh, Virginia, February 26, 1968, Technical Report.

Weeks, W. L. Electromagnetic Theory for Engineering Applications. John Wiley and Sons, Inc., New York, 1964, pp. 516-523.

Clarke, Kenneth K. "Fading Channel Simulators," Proceedings of the IEEE, 1966, pg. 83.

Chapin, E. W. and W. K. Roberts. "A Radio Propagation and Fading Simulator Using Radio-Frequency Acoustic Waves in a Liquid," Proceedings of the IEEE, 1966, pg. 1072.

COMPARISON OF REFLECTION TRANSMISSION COEFFICIENTS

Acoustics (Liq/Solid)	EMW (General)
$c^2 \quad \frac{\lambda + 2\mu}{\rho}$	$\frac{1}{\varepsilon\mu}$
C = Velocity of Propagation (longitudinal)	
b^2 = (shear) μ/f	
$\nabla^2\phi_{\ell_s} + k^2_{\ell_s}\phi_{\ell_s} = 0$	$\nabla^2 E + k^2 E = 0$
$\vec{V} = \nabla\phi + \nabla X\Psi$	$\vec{E} = -\nabla\phi + \frac{\partial\vec{A}}{\partial t}$

SNELL'S LAW

$k_1 \sin\phi_1 = k_1 \sin\phi_{11} = K_2 \sin\gamma_2$	$k_1 \sin\phi = k_{11} \sin\phi_{11} = k_2 \sin\phi_2$
$Z_\ell \quad Z_i = \rho c \sec\phi_1 \quad i = 1$	$\sqrt{\frac{\mu}{\varepsilon}} \sec\phi$ Vertical Polarization
$Z_{sh} = Z_t \quad \rho b \sec\gamma$	$\sqrt{\frac{\mu}{\varepsilon}} \cos\phi$ Horizontal Polarization
Reflection Coefficient (longitudinal) $V = \frac{Z_{tot} - Z_i}{Z_{tot} + Z_i}$, $i = 2$	$R = \frac{Z_2 - Z_1}{Z_2 + Z_1}$
Transmission Coefficient (longitudinal) $W = \frac{\rho}{\rho_1} \frac{2(Z_1 \cos 2\gamma_2)}{Z_{tot} + Z_1}$, $i = 2$	$T = \frac{2Z_2}{Z_1 + Z_2}$

Transmission Coefficient (shear) $= \frac{\rho}{\rho_1} \frac{2(Z_t \cos\gamma_2)}{Z_{tot} + Z_i} \quad i = 2$

$$Z_{tot} = Z_1 \cos^2 2\gamma_2 + Z_t \sin^2 2\gamma_2$$

$$Z_i = \rho_i C_i / \cos\theta_i \;, \quad Z_t = \rho_2 b_2 / \cos\gamma_2$$

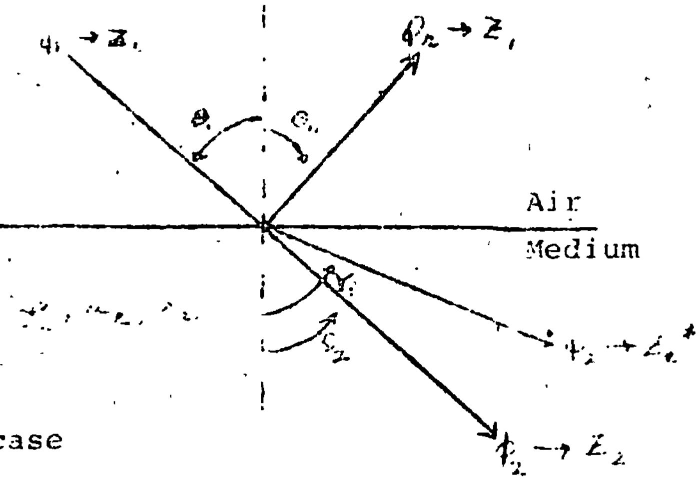

ℓ = longitudinal
Sh = Shear

*Only for acoustics case

Hook's Law

$[X_{ij}] = [C_{ij}][x_{ij}]$ strain

X_{ij} = stress in i to plane of application
j direction of applied force

$i = x_1 y_1 z$

$i = x_1 y_1 z$

$C_{ik} = C_{ki}$

$\Rightarrow$ 6 diag + 15 off diag = 21 constants

For isotropic case

$$[X_i] = [2a + \lambda, \lambda, \lambda][x_i]$$

$$X_1 = (2\mu+\lambda)x_1 + \lambda x_2 + \lambda_3 x_3 = 2a\ x_1 + \lambda(x_1+x_2+x_3)$$

μ, λ are Lame constants

APPROXIMATE [illegible] OF RCS MCS PEAKS
([illegible] RAT SCAT FACILITY PROJECT [illegible])

S.NO.	ANGLE°	DB
[illegible]	[illegible]	28.3
1	[illegible]	2[illegible]
2	4	2[illegible]
3	6	16.[illegible]
4	7	16.6
5	8	16.[illegible]
6	10	14.6
7	12	14.8
8	17.3	16.6
9	18	17.2
10	18.5	17.8
11	19	16.[illegible]
12	20	16.3
13	22	16.6
14	24.5	13.0
15	26.2	13.8
16	28	12.3
17	31	12.0
18	33	11.6
19	33.8	10.6
20	35	9.8
21	36	9.5
22	37	8.7
23	38	11.5
24	41	11
25	43	9.3
26	44	13
27	45.6	13
28	46	10.4
29	48	[illegible]
30	49	12.4
31	51	10.5
32	52	11.5
33	54	14.7
34	56	28.3
0	56	28.3
1	58	17.3
2	62	12.4
3	63	14.0
4	65	15.3
5	66	16.0
6	68	15.4
7	70	15.3
8	72	16.2
9	73	18.3
10	74	18.3
11	76.8	20.3
12	80	20.2
13	8[illegible]	15.4

S.NO.	ANGLE°	DB
14	83	16
15	85	13.0
16	88	12.5
17	89	17.0
18	90	36.0
0	90	36.0
1	94	17.6
2	95	13.5
3	96	15.6
4	99	17.5
5	101	20.6
6	102	21.4
7	107	17.0
8	108	18.7
9	110	19.5
10	112	16.5
11	114	16.5
12	116	13.6
13	118	14.4
14	120	17.6
15	121	16.0
16	124	21.8
17	126	20.3
18	127	18.5
19	128	20.5
20	132	22.0
21	134	19.7
22	135	18.5
23	136	15.6
24	138	16.3
25	140	21.0
26	142	19.5
27	144	19.4
28	145	21.5
29	146	22.5
30	148	19.6
31	150	23.2
32	152	23.6
33	154	16.5
34	158	25.3
35	160	25.3
36	161	23.7
37	163	27.0
38	166	27.0
39	167	28.3
40	168	27.5
41	170	28.3
42	172	31.5
43	174	25.7

S.NO.	ANGLE°	DB
44	176	31.8
45	177	33.0
46	180	41.1
0	180	41.1
1	182	33.5
2	184	28.2
3	186	31.3
4	187	32.2
5	189	31.5
6	190	27.9
7	192	27.5
8	193	31.5
9	194	30.5
10	195	27.0
11	197	28.1
12	199	30.5
13	201	23.5
14	203	26.8
15	207	21.0
16	209	26.5
17	210	23.0
18	212	21.0
19	213	23.3
20	216	24.0
21	218	20.7
22	222	23.3
23	223	23.2
24	225	20.0
25	228	22.0
26	230	24.7
27	232	23.5
28	233	20.3
29	235	17.3
30	237	21.9
31	238	21.5
32	240	17.5
33	242	16.7
34	244	19.6
35	245	22.8
36	248	22.5
37	250	24.0
38	251	23.0
39	252	23.0
40	254	21.2
41	257	19.8
42	258	18.5
43	261	16.5
44	263	13.3
45	265	12.5

S.NO.	ANGLE°	DB
46	26[illegible]	[illegible]
47	268	18.9
48	270	34.0
0	270	34.0
1	271	24.6
2	272	22.6
3	274	18.6
4	275	13.0
5	277	13.0
6	280	15.0
7	282	19.0
8	285	17.0
9	286	18.0
10	288	14.6
11	290	15.6
12	293	15.0
13	294	16.4
14	296	14.5
15	298	12.0
16	300	13.5
17	304	31.4
0	304	31.4
1	305	19.6
2	307	9.5
3	308	9.5
4	310	9.0
5	311	9.4
6	313	13.5
7	314	10.6
8	315	11
9	317	11
10	319	8.8
11	320	6.5
12	322	13.5
13	324	9.5
14	326	7.5
15	327	6.5
16	329	9.5
17	331	9.0
18	332	5.5
19	334	6.5
20	335	8.8
21	337	13.3
22	340	14.4
23	342	17.3
24	344	17.8
25	348	13.4
26	349	12.5

S.NO.	ANGLE°	DB
[illegible]	35[illegible]	[illegible]
28	352.5	13.[illegible]
29	352	1[illegible].4
30	354	15.[illegible]
31	355	18.[illegible]
32	357	23.[illegible]
33	360 or 0	28.[illegible]

APPROXIMATE COUNT OF RCS PEAKS
(AF-MDC-HDRT-RAT SCAT FACILITY PROJECT 6503)

S.NO.	ANGLE°	DB	S.NO.	ANGLE°	DB	S.NO.	ANGLE°	DB	S.NO.	ANGLE°	DB
0	[illegible]	27.2	50	54	13.2	0	90	34	50	125.9	21.3
1	.2	23.6	51	55	20.7	1	90.5	23.6	51	126	21.5
2	3.7	18	52	56	28.1	2	91	20.3	52	126.5	19.7
3	5	15.5				3	92	21	53	127.9	19.7
4	6	18.7	0	56	28.1	4	92.5	20.5	54	128	21
5	7.8	10.2	1	56.7	21.2	5	93	18.5	55	128.5	20.3
6	10	12.4	2	58	16.1	6	94	17.7	56	129.9	18.6
7	11	10.6	3	58.3	14.5	7	94.5	17	57	131	16.3
8	11.9	12.3	4	59	12.7	8	95	14.6	58	131.5	17.2
9	13	16.1	5	59.9	11.8	9	96.5	15	59	132.5	18.7
10	14.2	15.7	6	61.5	9.1	10	97	12.8	60	132.8	18.4
11	16	17.5	7	63	15.2	11	98.3	11.9	61	134	19.7
12	16.2	18	8	64.2	18.1	12	99	13.5	62	136.7	18.6
13	17	17.7	9	65	13.8	13	100	14.5	63	137.9	10.5
14	17.6	17.4	10	65.5	13.7	14	100.9	18.8	64	138.3	14.2
15	19	15.6	11	65.9	14.7	15	101	18.6	65	139	10.3
16	20.1	16.8	12	66	16	16	102	17.5	66	140.9	19.6
17	22	13.6	13	67	11	17	102.3	17	67	141	21.4
18	22.2	10.3	14	68	14.2	18	103.8	17.7	68	142.5	21.2
19	24.1	9.8	15	68.8	14	19	104.1	18	69	143	22.1
20	25.6	10.7	16	69	13	20	105	21.6	70	144	18.2
21	26	11.7	17	70.5	15.1	21	106	21.5	71	144.5	17.5
22	27	8.2	18	71	16.4	22	106.5	22.9	72	145	20.6
23	28	11.8	19	72	15.8	23	107	21.5	73	145.5	15.8
24	29	7.8	20	72.8	17.2	24	107.5	20.3	74	146.5	18.1
25	31	11.3	21	73	17.2	25	108	20.0	75	147	19.2
26	32.2	7.7	22	73.5	17.2	26	109	20.3	76	148.5	21.3
27	33	11.8	23	73.9	17.2	27	109.5	18.8	77	149	21.9
28	33.5	11.8	24	74.1	18.2	28	111	14.1	78	149.5	21
29	34.1	10.2	25	75	15.7	29	112.2	10.6	79	150.5	16.8
30	36	8.8	26	76	18.4	30	113	13.7	80	151	16
31	36.5	7.7	27	77	19.5	31	113.9	14.9	81	151.9	13.6
32	37	8.5	28	77.5	21.6	32	114.2	15.7	82	152.5	21.2
33	38.2	7.7	29	78.9	19.3	33	115	11	83	153.8	22.8
34	39.8	7	30	79	18.7	34	116	15.5	84	155.5	21.1
35	40.2	7.5	31	80	18	35	116.3	14.5	85	155.9	20.5
36	40.4	11.4	32	81	15.8	36	117	9.5	86	156.2	18
37	41	9.7	33	81.5	17.8	37	117.5	13.7	87	158.2	23.1
38	42	9.4	34	82.2	15	38	118	11.2	88	159	21.3
39	43	8.8	35	83.9	9.8	39	119	11.6	89	159.9	22.5
40	44	8.6	36	84.8	13.5	40	119.9	15.7	90	161	16
41	44.1	10.5	37	85.6	14	41	120.5	16.2	91	162	21.1
42	45.8	8.2	38	85.9	15.9	42	120.8	15.4	92	163	20.1
43	46	10	39	87	12.7	43	122	14.5	93	164	24.1
44	47	9	40	87.3	14	44	123	13.5	94	165	30.8
45	48	8.4	41	87.6	15	45	123.9	14.5	95	168	27.4
46	49.3	8.3	42	88	16.9	46	124	18	96	169	28.5
47	50	8.8	43	88.5	18.7	47	124.5	17.5	97	169.9	30.5
48	51	6.9	44	90	34	48	125	17	98	172.5	30.7
49	53	11.3				49	125.5	18.7	99	173	28.4

S.NO.	ANGLE°	DB	S.NO.	ANGLE°	DB	S.NO.	ANGLE°	DB
100	175	30.3	42	225.5	22.5	5	314	9
101	178	32.7	43	226	25	6	316	13.5
102	180	33	44	228	24.7	7	318	10.5
103	180.5	32.3	45	229	20.5	8	322	8
104	181	34.6	46	231	23	9	324	10.8
105	182	39.5	47	232	25	10	325	10.5
106	183	40	48	233	25.5	11	326	9.5
			49	236	21.5	12	329	9.7
0	180	41	50	238	20.5	13	330	13.5
1	181	37.1	51	240	22	14	332	8.5
2	182	32.3	52	242	23.5	15	333	11.5
3	183.9	33.1	53	243	22.5	16	335	11
4	184.5	31.1	54	246	21.8	17	337	11.5
5	186	27.8	55	248	22.8	18	338	12.5
6	187	28.1	56	250	25.5	19	340	16.8
7	189	35.2	57	252	22.8	20	341	16.7
8	190	33.6	58	254	22	21	342	15.5
9	191	29.5	59	256	22.6	22	345	14.9
10	193	28.6	60	259	18.9	23	347	14
11	194	28	61	262	18.5	24	349	14.5
12	195	32.5	62	265	18	25	352	11.5
13	196	28.8	63	267	15.6	26	354	13
14	199	22.4	64	268	17.5	27	357	25
15	200	29.6	65	270	34.5	28	359	28.3
16	200.5	25						
17	201.5	25.2	0	270	34.5			
18	202	21.5	1	272	20.5			
19	203	25.2	2	274	17.5			
20	204	25.2	3	276	14.5			
21	205	25.6	4	277	15.5			
22	206	22.3	5	279	16.5			
23	207	20.5	6	281	19.5			
24	208	21.2	7	284	15.5			
25	210	26.3	8	285	17.5			
26	212	24	9	290	15.0			
27	213.9	19.5	10	292	15.5			
28	214	17.1	11	293	16.5			
29	215	18	12	294	17			
30	216.1	20.7	13	295	13.5			
31	217	21	14	296	12.5			
32	219	20.1	15	297	13			
33	220	21.9	16	300	10.8			
34	220.2	21.7	17	302	16			
35	221	21.6	18	304	31			
36	221.9	22						
37	222	22	0	304	31			
38	223	16.1	1	306	9.5			
39	223.5	17	2	307	5.5			
40	224	18.7	3	309	10.5			
41	225	20.6	4	312	13.5			